Synthesis, Electrochemical, and Optical Properties of Low Band Gap Homo- and Copolymers Based on Squaraine Dyes

Sebastian F. Völker, Theresa Dellermann, Harald Ceymann, Marco Holzapfel, Christoph Lambert

Institut für Organische Chemie, Center for Nanosystems Chemistry, Universität Würzburg, Am Hubland, 97074, Würzburg, Germany

Correspondence to: C. Lambert (E-mail: christoph.lambert@uni-wuerzburg.de)

Received 21 October 2013; accepted 5 December 2013; published online 11 January 2014

DOI: 10.1002/pola.27073

ABSTRACT: A broad series of monomeric and polymeric squaraines was synthesized to investigate the impact of electron-donating bridges, such as unsaturated triarylamine, carbazole, and saturated piperazine groups, on the spectroscopic and redox properties. These bridges were attached to both standard *trans*-indolenine squaraines and dicyanomethylene-substituted *cis*-indolenine squaraines. The conjugates were investigated by absorption, steady-state, and time-resolved fluorescence spectroscopy and cyclic voltammetry. While addition of the donors resulted in significant redshift of the absorption of the model compounds, hardly any further shift or broadening was observed for the copolymers. Also the redox properties remained nearly unchanged compared with the model dyes. In contrast, immense broadening and redshift was observed for homopolymers. This behavior is explained by mostly excitonic coupling of localized squaraine transitions. The increasing distance of the chromophores determined by the bridges led to a decrease of the exciton coupling energy. We also performed semiempirical CNDO/S2 calculations on AM1 optimized structures. © 2014 Wiley Periodicals, Inc. J. Polym. Sci., Part A: Polym. Chem. **2014**, *52*, 890–911

KEYWORDS: conjugated polymers; dyes/pigments; synthesis

INTRODUCTION The use of functional dyes or π-conjugated polymers for optoelectronic and other applications requires fine-tuning of their optical and redox properties. In this paper we focus on the synthesis and some basic electronic (optical end electrochemical) properties of (co)polymers that are based on squaraine dyes combined with other electron donating π-conjugated building blocks such as carbazoles and triarylamines along with their monomeric parent compounds for comparison. This study shall provide a basis for using these polymers in optoelectronic devices in the future.

Squaraines represent a class of organic dyes that is related to cyanine dyes. The structure is similar, but, in contrast to cyanines, there is an additional electron accepting 3-oxocyclobut-1-enolate group centered in the middle. While cyanine dyes are positively charged, squaraines are zwitterionic and represent a donor-acceptor-donor structure. They are usually synthesized by 1,3-dicondensation reactions of squaric acid and nucleophilic compounds such as aniline derivatives, pyrroles or indolenine methylene bases and its heteroatom analogues. Squaraines are intensely colored and exhibit narrow and strong absorption ($\varepsilon > 10^5$ M^{-1} cm^{-1}) and emission in the red to near-infrared (NIR) region, similar to cyanines. For years, their suitability for various applications has been investigated. The potential as photoconductors in xerographic devices[1] has been studied as well as their application as materials for data imaging.[2] Furthermore squaraines can be used as fluorescence labels,[3–6] in nonlinear optics,[7–11] and in organic and hybrid photovoltaics.[12–19] Besides, their potential use as sensors for anions[20], cations,[21–24] and some neutral compounds[25,26] such as fructose[27] has been studied. Several excellent reviews give a deeper insight into chemistry and application of this class of dyes.[28–31]

There are various approaches to tune the properties of squaraine dyes. These properties strongly depend on the nucleophilic compound that is used in the squaraine synthesis. Moreover, the size of the π-system as well as the addition of further donor units at the periphery of the dyes shifts the absorption and emission towards lower energy. Also, replacement of one oxygen of the squaric carbonyl groups by dicyanomethylene,[13,32–34] sulfur,[33,35] or barbituric acid[33] for example leads to a significant change of the optical

Additional Supporting Information may be found in the online version of this article.

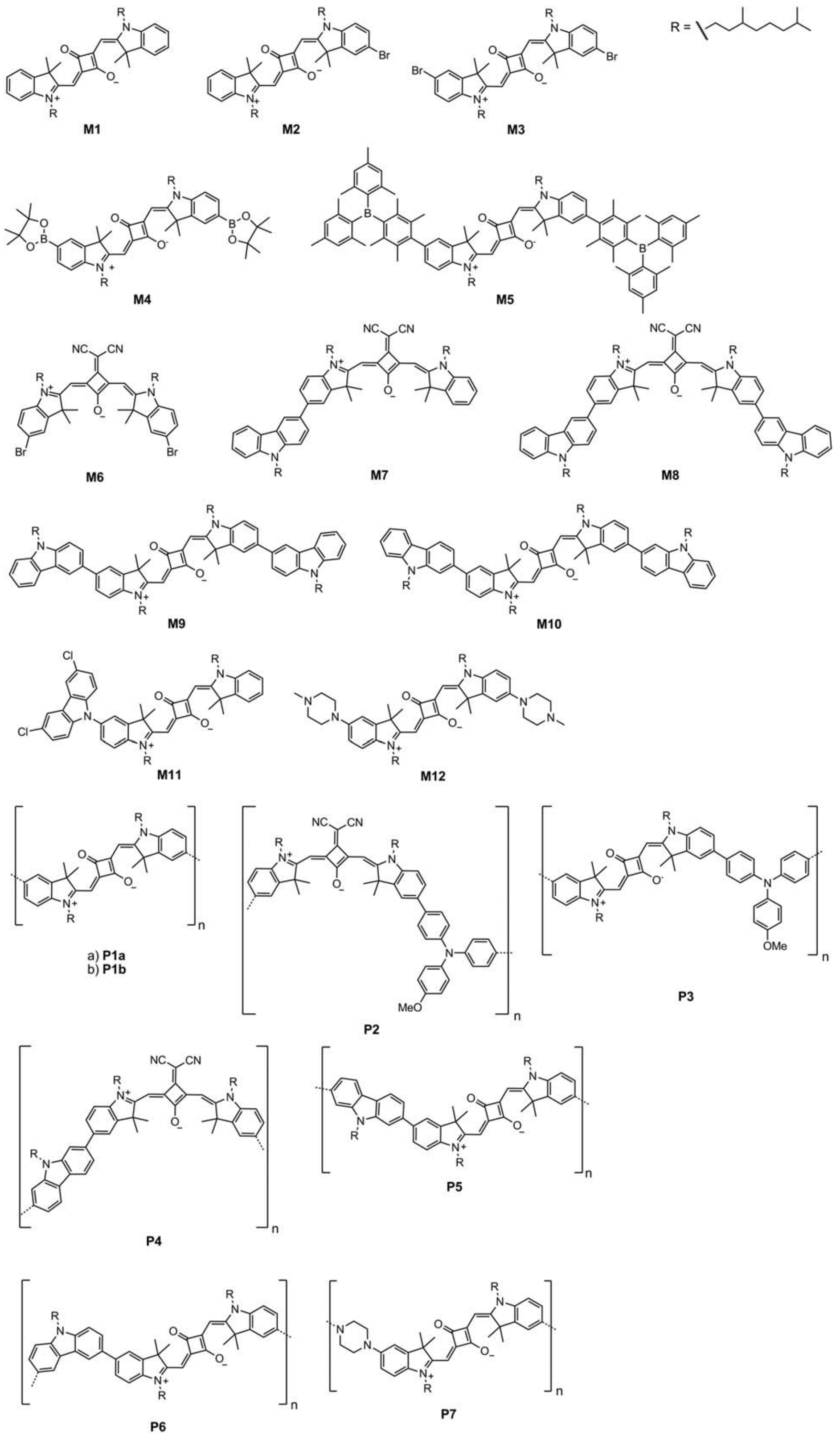

CHART 1 Target monomers **M1-M12** and polymers **P1-P7**.

properties. The stronger the electron accepting unit in the center of the squaraine dyes, the stronger is the induced bathochromic shift.

Another way to tune the optical properties of squaraines is the synthesis of oligomers and polymers where excitonic coupling of localized states leads to significant broadening

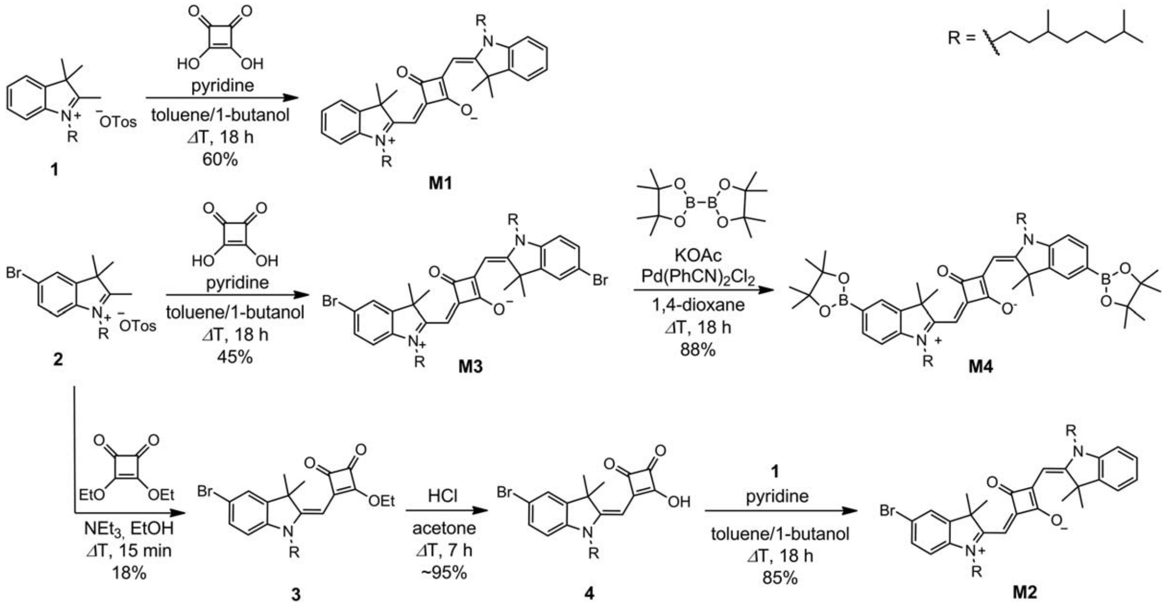

SCHEME 1 Synthesis of functionalized dyes **M1**-**M4**.

and shifts of the absorption. We recently synthesized some polymers where indeed the absorption spectra were considerably broadened and red-shifted.[14,34] Additionally there were contributions in the absorption at higher energy which could be explained by the concomitant existence of both H-type and J-type alignments of the chromophores that lead to hypsochromic and bathochromic shifts, respectively.

Historically, polysquaraines were the first squaraines to be reported about. Colored insoluble compounds were obtained by Treibs and Jacob upon condensation of squaric acid with pyrrole derivatives.[36,37] Since then, there have been numerous works on polysquaraines. Especially pyrrole-squaraine polymer derivatives have been extensively studied.[38,39] Furthermore, additional donor units such as fluorene or 2,5-dialkoxyphenylene were inserted into polysquaraines to obtain low-band-gap polymers with broad absorption in the NIR region.[40–42] Following this successful work, further donor components were inserted into 2,5-dialkoxyphenylene-pyrrole-squaraine polymers, such as 2,7-carbazole or thiophene derivatives which also resulted in polymers with a broad absorption in the NIR.[43,44]

In the field of indolenine-squaraines, only few approaches have been reported on the synthesis of donor-bridged squaraine copolymers. In search of polymers with broad absorption in the NIR region, Maeda et al. used both *meta-* and *para*-linked phenylene bridges but the bathochromic shift of the absorption was very small.[45] A similar behavior was observed by Kuster and Geiger where various bridges between indolenine-squaraines were investigated. In this work, a weak broadening and a small bathochromic shift of the absorption compared with monomeric model compounds was achieved even when 2,5-dialkoxyphenylene was used as the bridge.[46] However, Scherer et al. used thiophene groups to link indolenine-squaraines and synthesized a series of oligomers up to a pentamer. A significant redshift and broadening was found upon stepwise increase of the oligomer size.[11]

In this work here, we followed the idea of inserting additional very strong donor units into a polysquaraine system and synthesized a series of indolenine-squaraine copolymers with various electron rich bridging units. We used both saturated (piperazine) and unsaturated rigid (3,6- and 2,7-carbazoles) and propeller like (triarylamine) bridges to study their influence on the spectroscopic and electrochemical properties. Furthermore we likewise bridged squaraine dyes where an oxygen atom of the central carbonyl group was replaced by a dicyanomethylene group. Besides this, we also prepared some homopolymers and monomer conjugates for comparison (see Chart 1).

EXPERIMENTAL

Synthesis

The synthetic protocols can be found in the Supporting Information.

UV/Vis/NIR Spectroscopy

Ultraviolet/visible light/near-infrared spectra were measured using either a JASCO V670 or a Carey 5000 spectrometer. Compounds were dissolved in Uvasol solvents from Merck and measured in a concentration range of $\sim 10^{-5}$ to 10^{-7} M in 1 cm quartz cuvettes to exclude aggregate formation. The pure solvent was used as reference.

Fluorescence Spectroscopy

Fluorescence measurements were performed with a Photon Technology International (PTI) fluorescence spectrometer QM-2000-4 with a 75 W xenon lamp and a cooled photomultiplier (R928P) or a cooled InGaAs detector. The compounds

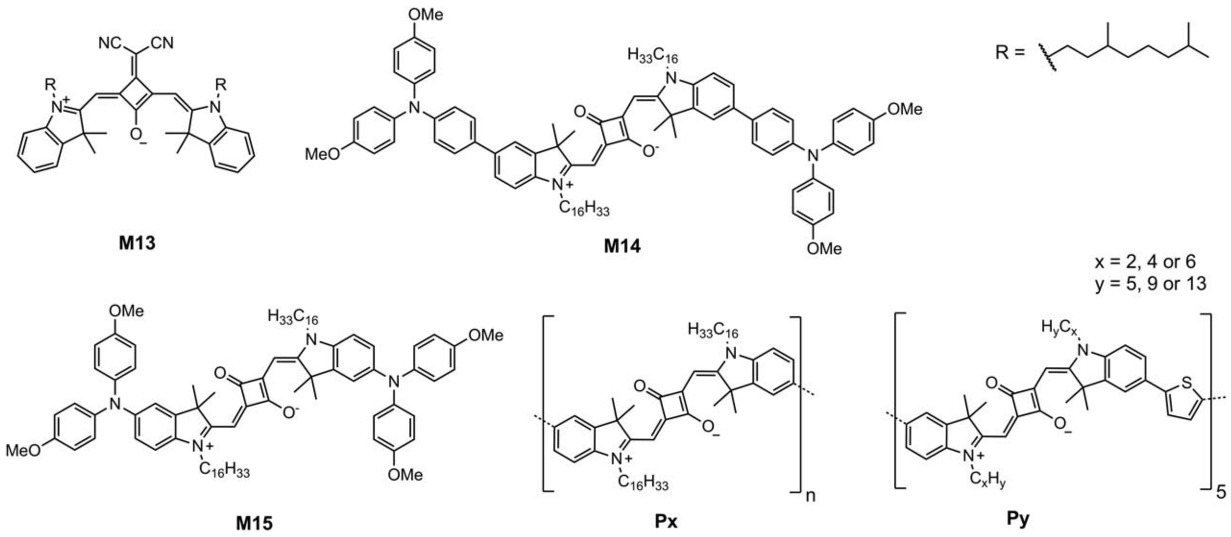

CHART 2 Previously published squaraine monomers **M13**[34], **M14**[50], **M15**[50] and polymers **Px**[14] and thiophene bridged pentamer **Py**.[11]

were dissolved in Uvasol solvents from Merck, purged with argon gas for 10 min and measured in 1 cm quartz cuvettes. As a fluorescence standard, Oxazine 1 in ethanol ($\phi_{\mathrm{fl}} = 0.11$) was used and the following equation was applied to determine the quantum yields.[47]

$$\phi_{\mathrm{fl}} = \phi_{\mathrm{fl,Ref}} \left(\frac{I(\tilde{\nu}) \times OD_{\mathrm{Ref}} \times (n_{\mathrm{D}}^{20})^2}{I(\tilde{\nu})_{\mathrm{Ref}} \times OD \times (n_{\mathrm{D}}^{20})^2_{\mathrm{Ref}}} \right)$$

where ϕ_{fl} is the quantum yield of the sample, $\phi_{\mathrm{fl,Ref}}$ is the quantum yield of the reference, $I(\tilde{\nu})$ the integrated emission band, OD the optical density of the absorption band at the excitation wavelength, and $n_{\mathrm{D}}{}^{20}$ is the refraction index of the solvent.

Fluorescence Lifetimes

The samples, that were prepared likewise to the steady state fluorescence measurements, were excited with a 650 nm laser diode and measured with a PTI TM-2/2003 fluorescence lifetime spectrofluorometer. To determine the instrument response (~1.5 ns) we used colloidal silica in deionised water as scatter solution. The lifetimes were obtained after fitting of the decay curves with exponential decay functions.

Cyclic Voltammetry

Cyclic voltammetric measurements were performed in DCM, THF or $CDCl_3$ with tetrabutylammonium hexafluorophosphate (TBAHFP) (0.2 M) as supporting electrolyte. We used a three electrode setup with a platinum working electrode (ø 1 mm), a helical platinum counter electrode and either a platinum pseudo reference electrode or an Ag/AgCl "leak free" reference electrode[48] in a completely sealed and with argon flushed glass vessel. In case of the platinum pseudo reference electrode, the potentials were measured against the redox couple of decamethylferrocene/decamethylferrocenium and calculated against the ferrocene/ferrocenium (Fc/Fc^+) redox couple.[49]

Gel permeation Chromatography (GPC)

All measurements were performed at 20 °C in chloroform with a Shimadzu instrument (diode array detector SPD-M20A, system controller CBM-20A, solvent delivery unit LC-20AD, on-line degasser DGU 20A9). Preparative chromatography was carried out in recycling mode on two consecutive SDV columns (50 Å and 500 Å, dimension: 20 × 600 mm, particle size: 10 μm) from PSS. Analytical chromatography was carried out on a SDV column (analytical linear S mixed bed, dimension: 8 × 300 mm, particle size: 5 μm) from PSS with polystyrene as standard.

RESULTS AND DISCUSSION

Synthesis

Squaraine Dye Building Blocks

For a thorough investigation of the impact of the various substitutions on the squaraine dyes, a completely nonfunctionalized dye is necessary as well as functionalized dyes for further syntheses. Therefore we synthesized **M1** (Scheme 1)

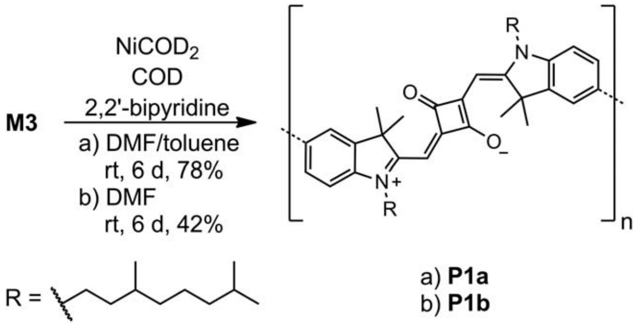

SCHEME 2 *Yamamoto* coupling to the homopolymers **P1a** and **P1b**.

TABLE 1 Polymer Characterization: Number-Average Molecular Weight (M_n), Number Average Degree of Polymerization (X_n), Weight-Average Molecular Weight (M_w), and Polydispersity (M_w/M_n)[a]

	M_n	X_n	M_w	M_w/M_n
P1a	31,000	45.9	80,200	2.59
P1b	8,100	12.0	22,700	2.81
P2	14,700	14.7	31,900	2.17
P3	15,800	16.7	32,800	2.07
P4	13,700	13.3	73,200	5.35
P5	20,900	21.4	61,500	2.94
P6	6,200	6.4	20,600	3.30
P7	9,400	12.4	28,800	3.07

[a] Analysis was performed in $CHCl_3$ with polystyrene as standard.

which does not comprise any bromine substituents or other functional groups at the periphery, the mono- and dibrominated dyes **M2** and **M3**, respectively, as well as the boronic ester derivative **M4**.

We started with the quaternary salts **1** and **2**, whose synthesis is described in a previous publication.[34] In situ deprotonation with pyridine to the highly nucleophilic methylene bases and subsequent reaction with squaric acid in a solvent mixture of 1-butanol and toluene (1:1) with azeotropic distillation of water using a Dean-Stark trap, resulted in the nonfunctionalized and dibrominated squaraine dyes **M1** and **M3**, respectively.

The bromine atoms in **M3** were substituted by boronic ester groups via the Pd-catalyzed *Miyaura* borylation reaction using bis(pinacolato)diboron, $Pd(PhCN)_2Cl_2$ and 1,1′-bis(diphenylphosphino)ferrocene (dppf), resulting in **M4** in high yields.

The monobrominated asymmetric dye **M2** was obtained after three steps from the quaternary salt **2** which was condensed with 3,4-diethoxy-3-cyclobutene-1,2-dione in the presence of NEt_3 in boiling ethanol to the semisquaraine **3** which was almost quantitatively hydrolyzed under acidic conditions to the acidic form **4**. Further condensation reaction with the quaternary salt **1** in toluene and 1-butanol yielded the asymmetric dye **M2**.

Squaraine Homopolymers

In analogy to our previous work, we synthesized squaraine homopolymers based on monomer **M1**.[14] Since polyindolenine squaraine **Px** (= **P1** with $R = C_{16}H_{33}$, Chart 2) was only soluble in $CHCl_3$ and solvent mixtures consisting of both a chlorinated solvent and an alcohol, we replaced the linear alkyl chain of polymer **Px** by a branched 3,7-dimethyloctyl chain hoping to increase the solubility.

The Ni-mediated *Yamamoto* coupling reaction of **M3** was carried out under the same conditions as for **Px** (Scheme 2), namely stirring at room temperature for six days in a solvent mixture of DMF and toluene (1:1). The resulting polymer **P1a**, with a number average molecular weight of $M_n = 31{,}000$ and a degree of polymerization of $X_n = 46$, precipitated out of the solution during the reaction. This polymer **P1a** is ∼30% longer than our previous polymer **Px** ($X_n = 33$), but solubility was again restricted to $CHCl_3$ and the aforementioned solvent mixtures.

Because **P1a** proved poorly soluble in pure solvents, we used pure DMF as the solvent for the *Yamamoto* coupling of **M3** under elsewise identical reaction conditions to provoke precipitation of the polymers at an earlier stage of polymerization condensation reaction to get shorter and thus possibly better soluble polymers. Indeed, this reaction resulted in lower yield but also in the shorter polymer **P1b** ($M_n = 8100$, $X_n = 12$) with increased solubility (soluble in pure DCM and pure PhCN for example). All analytical GPC data for determining the polymer mass distribution can be found in Table 1.

Triarylborane Substituted Squaraine Monomer

To investigate the impact of additional acceptor units at the periphery of the dye molecule, we attached triarylboranes, where the boron center is protected by six methyl groups (**M5**, Scheme 3). These acceptor-squaraine-acceptor dyes are topologically similar to the donor-squaraine-donor dyes which we recently investigated.[50] For the synthesis of **M5**, overnight heating of **M4** and triarylborane **5**, which was synthesized from 1,4-dibromo-2,3,5,6-tetramethylbenzene and dimesitylfluoroborane according to literature

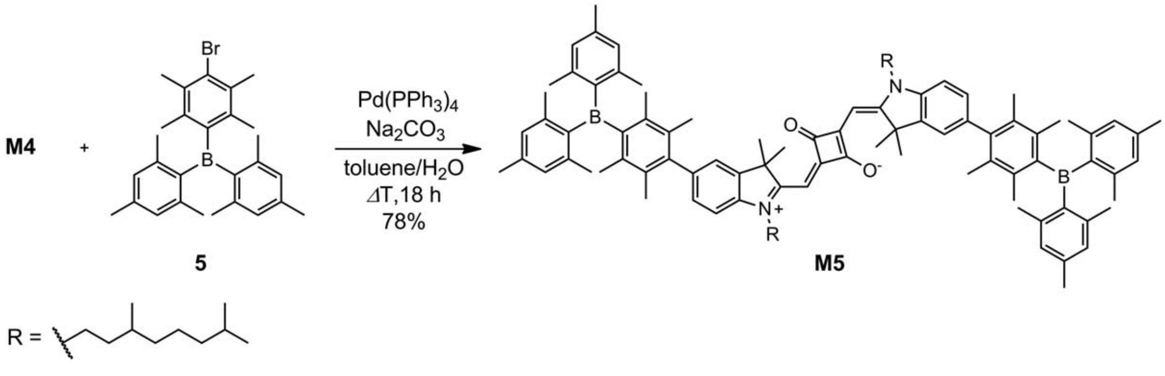

SCHEME 3 Synthesis of triarylborane substituted squaraine dye **M5**.

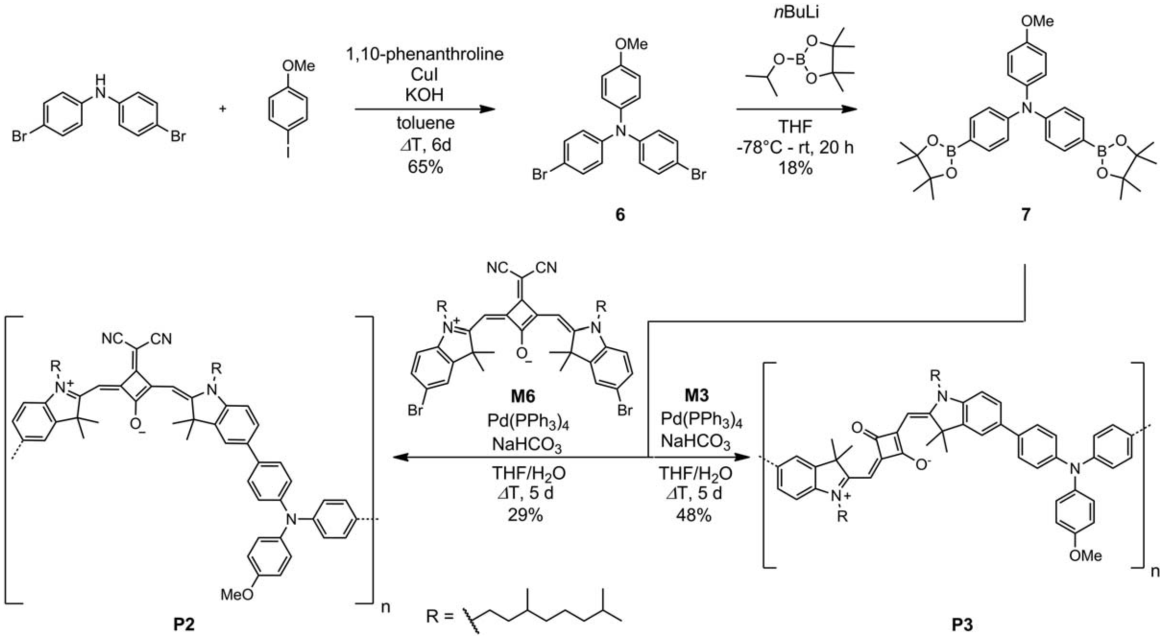

SCHEME 4 Synthesis of triarylamine precursor and the copolymers **P2** and **P3**.

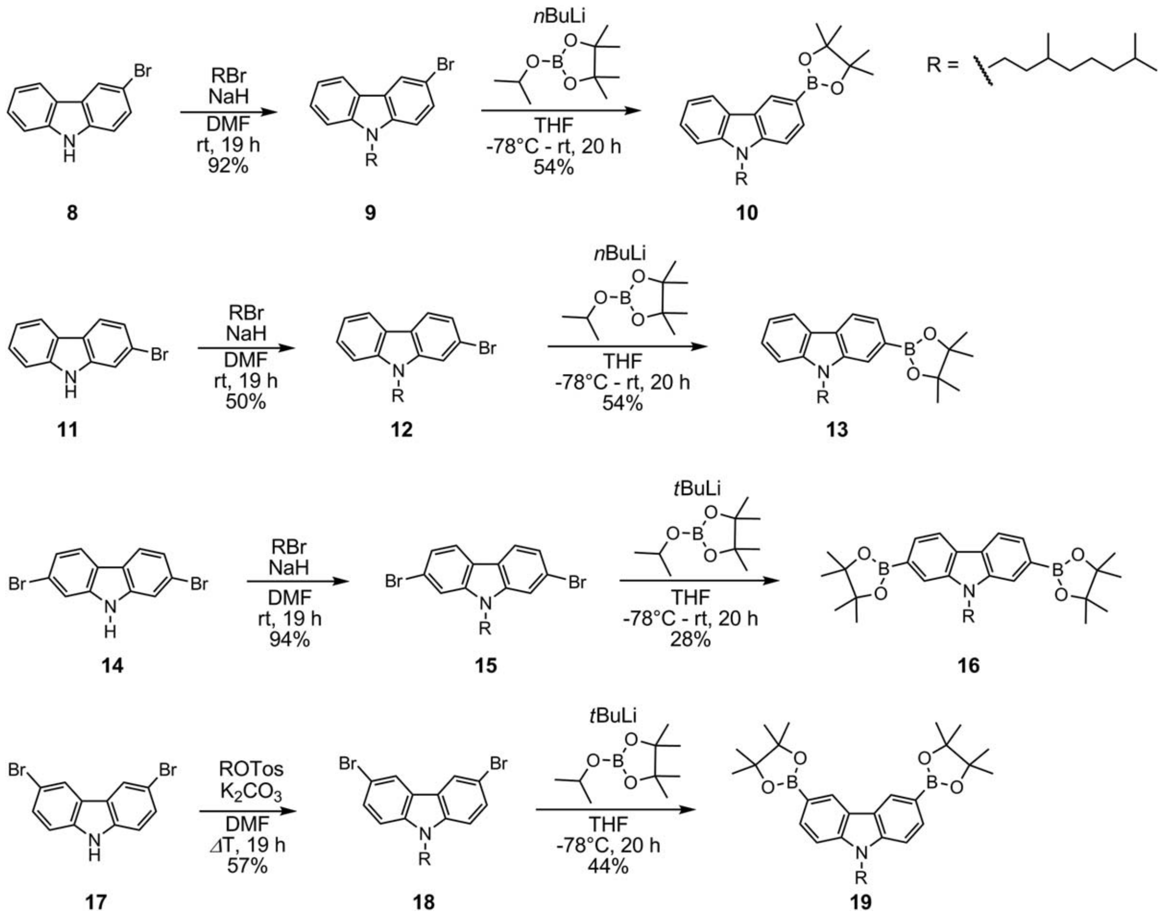

SCHEME 5 Synthesis of carbazole precursors.

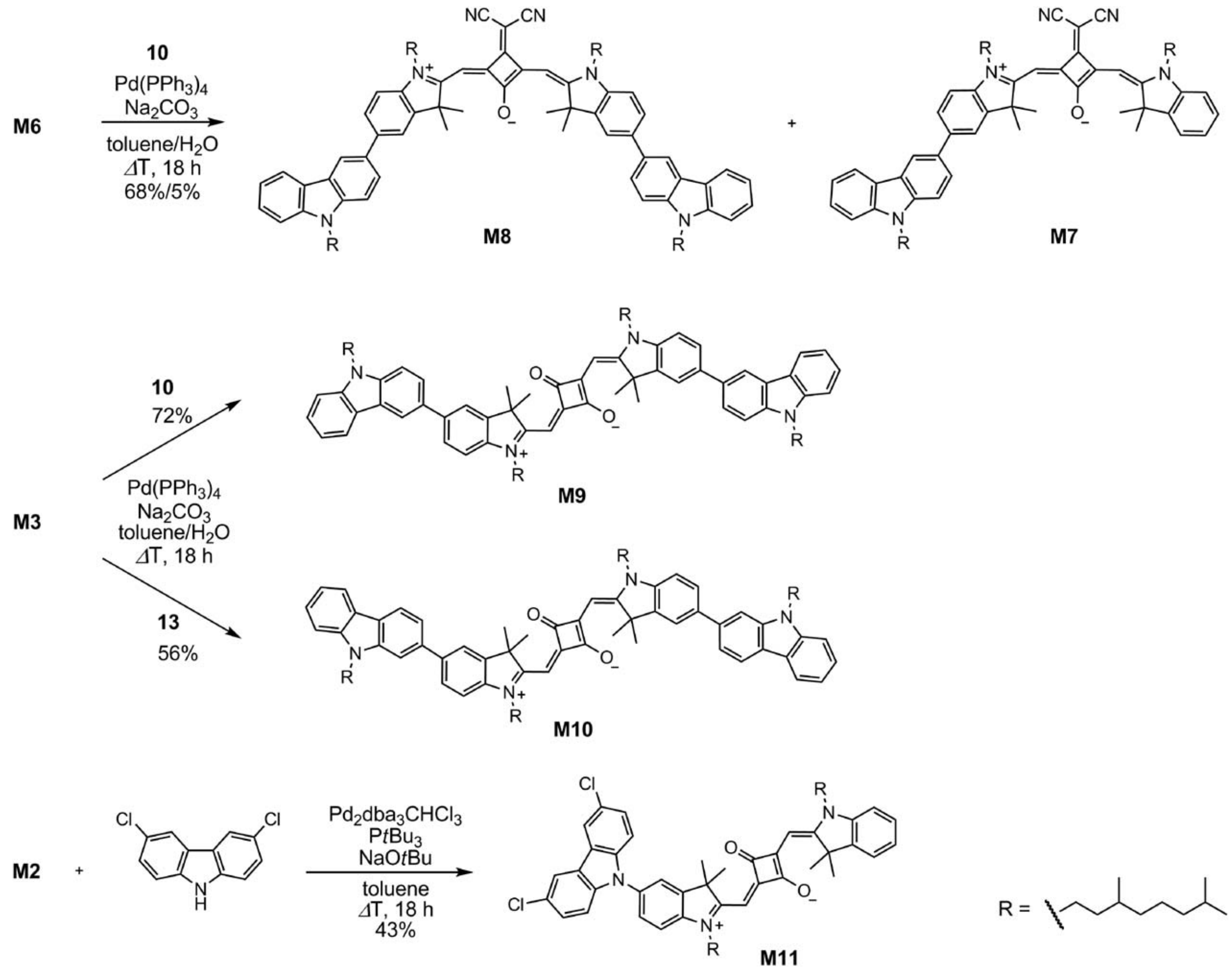

SCHEME 6 Synthesis of carbazole substituted squaraine dyes.

procedures,[51] with $Pd(PPh_3)_4$ and Na_2CO_3 in a solvent mixture of toluene and water resulted in **M5** in high yield.

Donor Substituted Squaraines

Following our previous work on donor substituted squaraine dyes,[50] we synthesized various copolymers using triarylamine (Scheme 4), carbazoles (Scheme 7) and a non-conjugating piperazine (Scheme 8) as bridging units as outlined below:

Triarylamine Squaraine Copolymers

The triarylamine precursor **7** was synthesized in two steps applying the copper catalyzed *Ullmann* coupling of *bis*(4-bromophenyl)amine and 1-iodo-4-methoxybenzene to **6** in the first step (Scheme 4). Halogen-metal exchange with *n*BuLi and subsequent addition of the borolane eventually gave the diboronic ester **7** in low yield. Copolymerizations of **7** with either **M3** or the previously published **M6**[34] were carried out by continuous heating in THF/water for five days to give the copolymers **P3** and **P2**, respectively. Both polymers are of similar size with a degree of polymerization $X_n \sim 15$. However, in case of **P3** solubility turned out to be poor. A major part of the polymer was insoluble in common organic solvents. Therefore the fraction we used for all the physical characterizations throughout this work was the part that remained insoluble during treatment in a Soxhlet apparatus with DCM but dissolved when replacing DCM by $CHCl_3$.

Carbazole Substituted Squaraines

Triarylamines possess a propeller-like structure which shows some flexibility.[52] In order to increase conjugation, we replaced the triarylamine by the more rigid carbazole bridge which was connected either via its 2- or 3- position to the squaraines.

The synthesis of the carbazole precursors is straight forward (Scheme 5). All non-alkylated brominated carbazoles were synthesized according to literature procedures. Deprotonation of the mono-(**8**[53], **11**[54]) or dibrominated (**14**[55], **17**[56]) carbazoles with either NaH or K_2CO_3 and subsequent alkylation with 3,7-dimethyloctyl bromide or tosylate in DMF gave the alkylated carbazoles **9**, **12**, **15**, **18** in moderate to very good yields. The boronic ester was attached via halogen-lithium exchange in THF, using *n*BuLi for the monobrominated and *t*BuLi for the dibrominated species, and subsequent addition of the borane to give the boronic esters **10**, **13**, **16** and **19**.

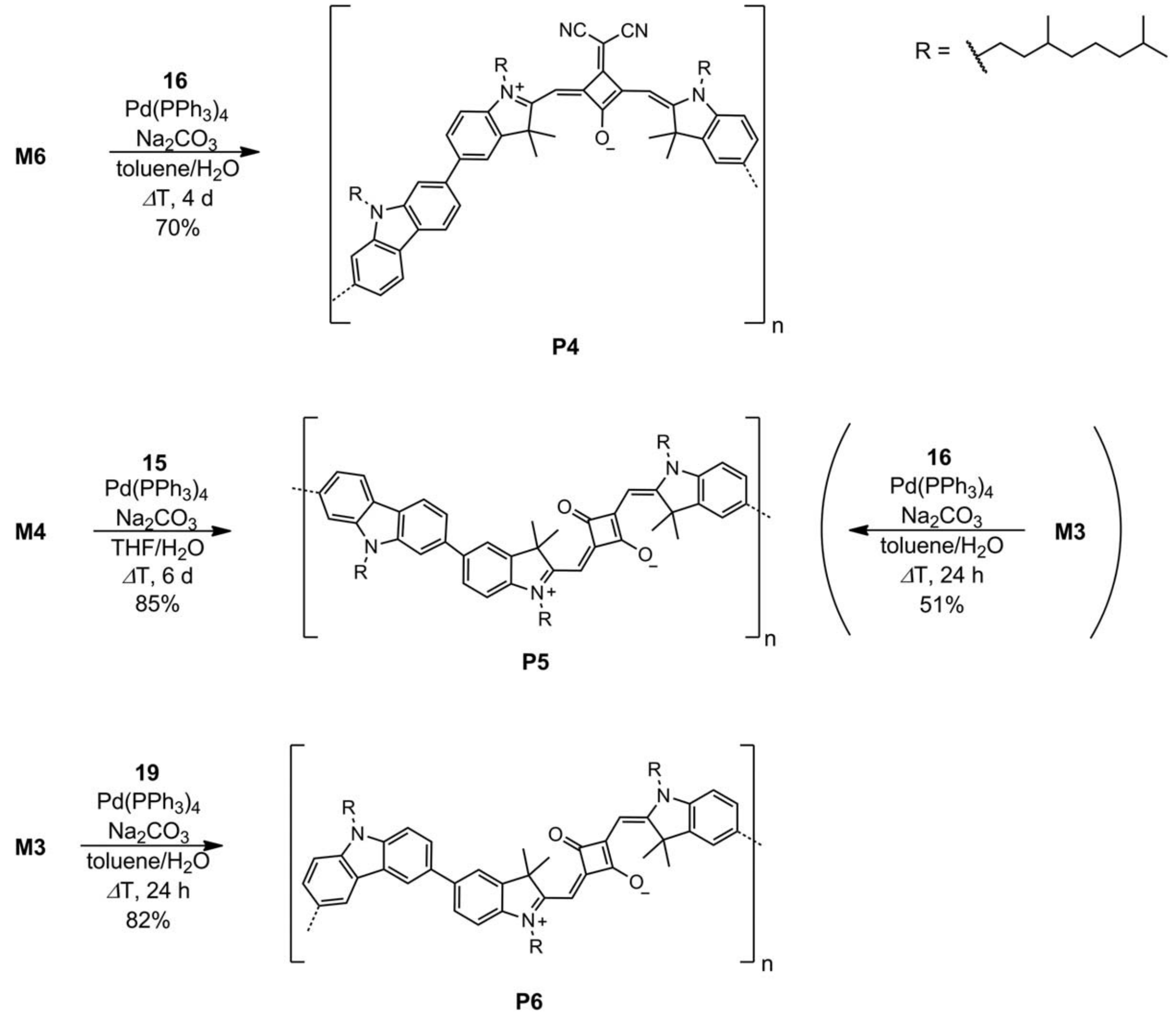

SCHEME 7 Synthesis of carbazole-squaraine copolymers.

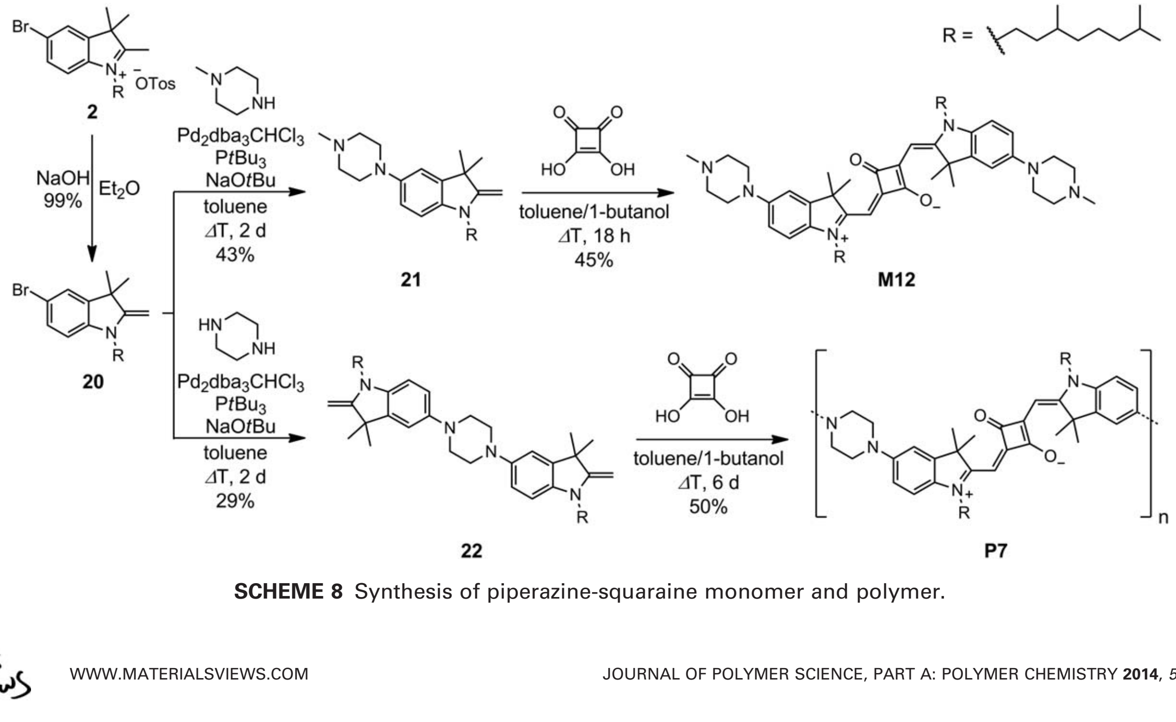

SCHEME 8 Synthesis of piperazine-squaraine monomer and polymer.

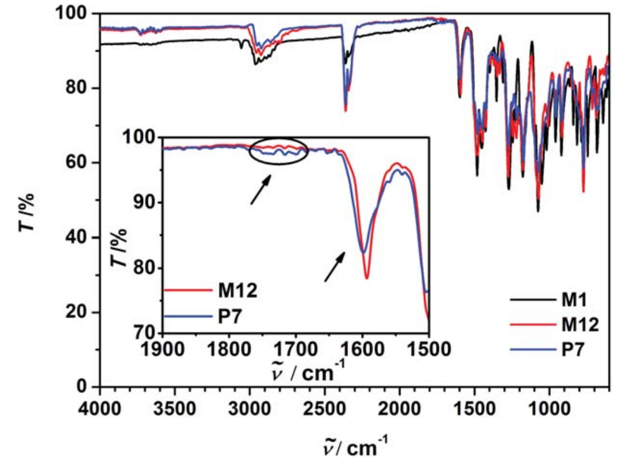

FIGURE 1 Complete IR spectra of **M1**, **M12** and **P7** and magnified spectra of **M12** and **P7** (inset).

Suzuki coupling of squaraine **M6** with carbazole **10** in toluene/water (Scheme 6) gave both mono- and disubstituted squaraines **M7** and **M8**, respectively, after careful separation by preparative recycling GPC. Squaraine **M3** was coupled with both **10** and **13** to yield the substituted squaraines **M9** and **M10**, respectively, to investigate the impact of the different linking positions of the carbazoles.

We also connected a carbazole unit via its *N*-position to a squaraine dye which yields an asymmetric dye conjugate for potential future purposes. *Buchwald-Hartwig* coupling reaction of monobrominated squaraine **M2** with 3,6-dichloro-9*H*-carbazole gave substituted squaraine **M11**. In this reaction, the temperature plays a particularly crucial role. Under refluxing conditions the product could not be isolated. We always found mixtures with substances where additional carbazole units were coupled to the one that was already attached at the squaraine core. This could be avoided by reducing the temperature to 80 °C for a reaction time of 18 h.

Carbazole Squaraine Copolymers

The reaction of squaraine **M6** with carbazole **16** in toluene/water resulted in polymer **P4** with reasonable yield and mass distribution ($M_n = 13{,}700$, $X_n = 13$), whereas the same reaction conditions for dibromosquaraine **M3** and carbazole diboronic ester **16** only gave low yield and much shorter polymers **P5** ($M_n = 7090$, $X_n = 7.2$) (see Scheme 7). This is most likely due to the precipitation of shorter polymer strands during reaction in this particular solvent mixture after a couple of hours. However, the reaction of squaraine diboronic ester **M4** with dibromocarbazole **15** in THF/water proceeded very well to give longer polymers **P5** ($M_n = 20{,}900$, $X_n = 21$) in higher yield. This load of the longer polymers **P5** was used for the characterization throughout this work. The copolymerization reaction for **M3** and 3,6-disubstituted carbazole **19** in toluene/water with Na_2CO_3 gave good yields but short polymers **P6** ($M_n = 6200$, $X_n = 6.4$). The synthetic approach in THF/water, analogous to the synthesis of **P5**, was not pursued in this case, because no major differences neither of the optical properties between the 2,7-carbazole or 3,6-carbazole bridged copolymers nor of the optical and electrochemical properties of the monomeric model compounds were observed.

TABLE 2 Redox Potentials (vs. Ferrocene/Ferrocenium) and Band Gaps of Monomers Determined by Both Cyclic Voltammetry (E(gap)^{CV}) and Absorption Spectroscopy (E(gap)^{opt})

	Solvent	3rd red $E_{1/2}$ (mV)	2nd red $E_{1/2}$ (mV)	1st red $E_{1/2}$ (mV)	1st ox $E_{1/2}$ (mV)	2nd ox $E_{1/2}$ (mV)	3rd ox $E_{1/2}$ (mV)	4th ox $E_{1/2}$ (mV)	HOMO[a] (eV)	LUMO[a] (eV)	E(gap)^{CV}[a] (eV)	E(gap)^{opt}[b] (eV)
M1	THF[c]		−2631[d]	−1660	64	442			−5.32	−3.60	1.72	1.88
M6	THF[e]		−2312[d]	−1320	245				−5.51	−3.94	1.57	1.71
M5	THF[e]	−2647[d]	−2487[d]	−1655	64	454			−5.32	−3.61	1.71	1.84
M4	DCM[e]			−1678	71	524			−5.23	−3.48	1.75	1.85
M7	DCM[c]			−1502	146	570	802[d]		−5.31	−3.66	1.65	1.69
M8	DCM[c]			−1468	96	542			−5.26	−3.69	1.57	1.65
M9	DCM[c]			−1670	1	523			−5.16	−3.49	1.67	1.77
M10	DCM[c]			−1653	35	544			−5.20	−3.51	1.69	1.79
M11	DCM[c]			−1701	88	557	1151		−5.25	−3.46	1.79	1.86
M12	DCM[e]			−1711	−214	231	994[d]		−4.95	−3.45	1.50	1.73
M14[50]	DCM[c]			−1664	−6	277	277	587	−5.16	−3.51	1.65	1.75
M15[50]	DCM[c]			−1717	−190	221	491	833	−4.98	−3.45	1.53	1.65

[a] Obtained from the half wave potentials of cyclic voltammetry measurements. All redox potentials are given versus Fc/Fc$^+$ which has a potential of 0.46 eV in TBAHFP/DCM and in TBAHFP/THF 0.56 eV versus saturated calomel electrode (SCE).[61] The potential of SCE is 0.244 V versus the normal hydrogen electrode (NHE),[62] which has an absolute potential of 4.46 eV versus vacuum.[63] Therefore, in DCM $E(\text{HOMO/LUMO}) = -5.16$ eV – $E_{1/2}$(1st ox/1st red) and the electrochemically derived band gap is $E(\text{gap})^{CV} = E(\text{LUMO}) - E(\text{HOMO})$. In THF, the absolute potential of Fc/Fc$^+$ has to be replaced by −5.26 eV.

[b] Determined in DCM by the intersection point of a tangent on the inflexion point of the low energy side of the absorption band and the *x*-axis.

[c] Platinum pseudo reference electrode.

[d] Potentials extracted from DPV.

[e] Ag/AgCl "leak free" reference electrode.

TABLE 3 Redox Potentials (vs. Ferrocene/Ferrocenium) and Band Gaps of Monomers Determined by Both Cyclic Voltammetry ($E(\text{gap})^{\text{CV}}$) and Absorption Spectroscopy ($E(\text{gap})^{\text{opt}}$)

	Solvent	1st red $E_{1/2}$ (mV)	1st ox $E_{1/2}$ (mV)	2nd ox $E_{1/2}$ (mV)	3rd ox $E_{1/2}$ (mV)	4th ox $E_{1/2}$ (mV)	HOMO[a] (eV)	LUMO[a] (eV)	$E(\text{gap})^{\text{CVa}}$ (eV)	$E(\text{gap})^{\text{optb}}$ (eV)
P1b	DCM[c]	−1,671	62	570			−5.22	−3.49	1.73	1.63
P2	DCM[d]	−1,466	112	407	607		−5.27	−3.69	1.58	1.62
P3	$CDCl_3$[c]	–	25[e]	325[e]	465[e]	843[e]	–	–	–	(1.68)/1.74
P4	DCM[d]	−1,454	147	563			−5.31	−3.71	1.60	1.63
P5	DCM[d]	−1,656	60	530			−5.22	−3.50	1.72	1.76
P7	DCM[d]	−1,744	−183	219			−4.98	−3.42	1.56	(1.54)/1.72

[a] Obtained from the half wave potentials of cyclic voltammetry measurements. All redox potentials are given versus Fc/Fc^+ which has a potential of 0.46 eV in TBAHFP/DCM and in TBAHFP/THF 0.56 eV versus saturated calomel electrode (SCE).[61] The potential of SCE is 0.244 V versus the normal hydrogen electrode (NHE)[62], which has an absolute potential of 4.46 eV versus vacuum.[63] Therefore, in DCM $E(\text{HOMO/LUMO}) = -5.16\ \text{eV} - E_{1/2}(\text{1st ox/1st red})$ and the electrochemically derived band gap is $E(\text{gap})^{\text{CV}} = E(\text{LUMO}) - E(\text{HOMO})$. In THF, the absolute potential of Fc/Fc^+ has to be replaced by −5.26 eV.

[b] Determined in $CHCl_3$ by the intersection point of a tangent on the inflexion point of the low energy side of the absorption band and the *x*-axis, the values in brackets were obtained when the tangent was placed on the low energy shoulder of the main absorption band.

[c] Platinum pseudo reference electrode.

[d] Ag/AgCl "leak free" reference electrode.

[e] Potentials extracted from DPV.

Piperazine-Squaraine Monomer and Copolymer

Piperazine was chosen as a nonconjugating electron donor that may be used as a bridge to connect squaraine dyes. Because the *Buchwald-Hartwig* coupling reaction did not prove successful for the polymerization step for a similar system in our lab, a different synthetic route was followed where the piperazine was attached to the methylene base before the dye condensation synthesis (Scheme 8).

In the first step, the quaternary indolenine **2** salt was quantitatively deprotonated to give the highly nucleophilic methylene base **20**. Thereafter, analogous reaction sequences were used to synthesize both the model compound and the copolymer. *Buchwald-Hartwig* reaction of the methylene base **20** with *N*-methylpiperazine gave **21** which was treated with squaric acid in a condensation reaction to yield the model compound **M12** in moderate yield. For the polymer precursor, **20** was coupled twice with piperazine to give **22**. Here, immediate recrystallization of the crude product from ethanol proved essential to prevent the product from further side reactions. Polymerization was then carried out analogous to the monomer squaraine condensation synthesis in toluene/1-butanol (1:1) using a Dean-Stark trap. However, the polycondensation reaction was carried out under nitrogen atmosphere and the reaction time was extended to six days to obtain polymer **P7** ($M_n = 9400$, $X_n = 12$).

Physical Characterization

Molecular Weight Distribution

Molecular weight distributions of all isolated polymers were determined by analytical GPC using polystyrene standards (see Table 1). In general the degree of polymerization X_n depends on the solubility of the polymer under the given reaction conditions and varies from about 7 up to 45. The polydispersity $\text{PDI} = M_w/M_n$ varies between 2 and 5 typical of polycondensation reactions which should ideally show a Flory distribution with PDI = 2. The deviation from this values can be understood by the work up extraction procedures which remove both very short (=very soluble) and very long (=insoluble) polymer fractions from the crude polymer product.

IR Spectroscopy

It is well known that in the condensation reaction of a squaric acid derivative with nucleophilic compounds the central ring can be disubstituted both in the 2,4-positions to the squaraine dye and in 3,4-positions of a cyclobutenedione compound.[57–59] The solvent that is used in this condensation reaction step plays a crucial role, e.g. the use of a toluene/1-butanol solvent mixture usually gives 2,4-substituted products only. In the case of monomeric squaraine dyes, even traces of 3,4-substituted products can be removed via flash chromatography to give pure 2,4-isomeric squaraine products. A subsequent transition metal catalyzed or mediated polycondensation reaction therefore will give polymers with only isomerically pure squaraine subunits where the central ring is disubstituted at the 2,4-positions. However, this may be different in cases where the squaraine forming reaction is the polycondensation step itself as for the bifunctional methylene base **22** and squaric acid to form **P7**. Therefore, even though it is unlikely, the formation of 3,4-substituted subunits cannot be completely ruled out. To prove their absence, we used IR spectroscopy. In case of 3,4-substitution, a diketone structure of the cyclobutene ring shows a C=O vibration at around 1680 to 1800 cm^{-1}.[60] Due to the delocalized character of 2,4-substituted units, this vibration is not observed in this case, but a vibration of the delocalized central C=C double bonds at around 1600 cm^{-1} should be seen. Thus, IR spectra of polymer **P7** and, for comparison, of monomers **M12** and **M1** were recorded. Figure 1 shows the complete IR spectra and a magnified part of **M12** and **P7** (inset). As can be seen for the monomers, there is absolutely no signal at around 1680 to 1800 cm^{-1}. For the polymer very

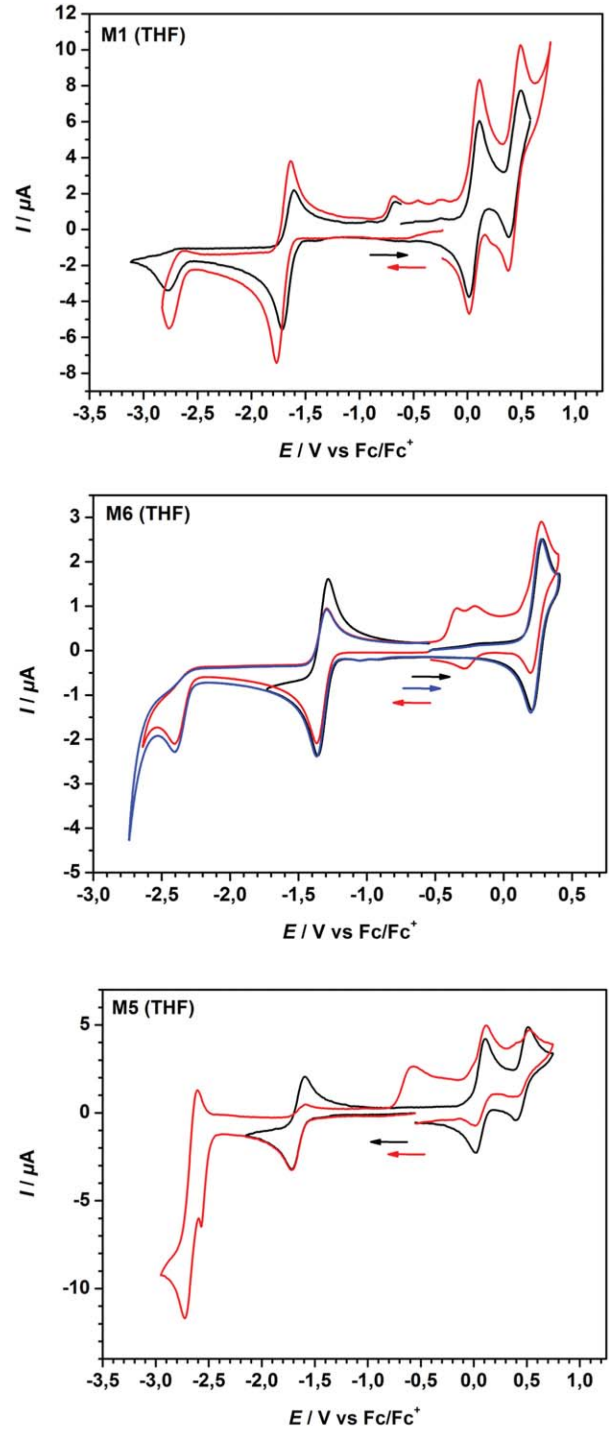

FIGURE 2 Cyclic voltammograms of **M1**, **M6** and **M5** in TBAHFP/THF (0.2 M) at a scan rate of 250 mV s^{-1}.

weak bands in this region indicate indeed negligible formation of 3,4-substituted squaraine moieties.

Cyclic Voltammetry

Monomers

Cyclic voltammetry (CV) measurements were performed in DCM for most squaraine monomers and polymers. Due to solubility issues, **P3** was measured in $CDCl_3$. In cases in which the reduction is of particular interest (such as **M5**), CVs were measured in THF. All data of the monomers and polymers can be found in Tables 2 and 3 and selected CVs in Figure 2 to 7.

In addition to the reduction and two oxidation processes that are common for indolenine-squaraine dyes (**M1, M6**),

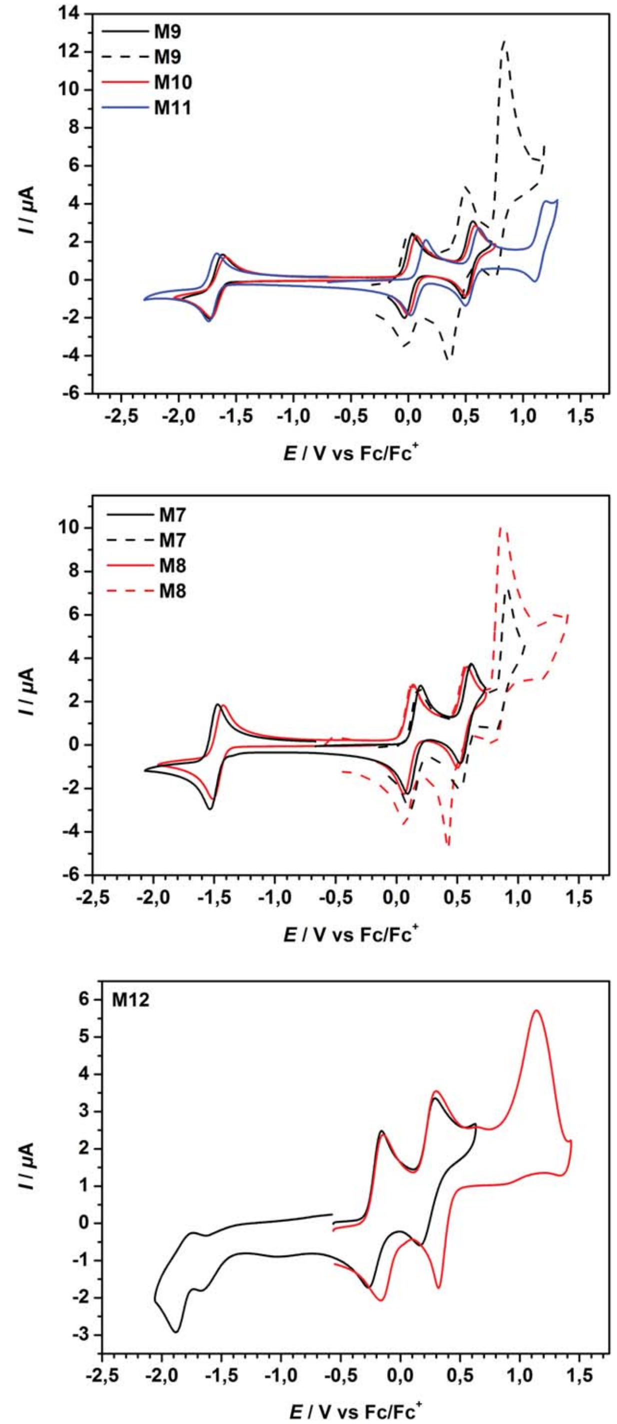

FIGURE 3 Cyclic voltammograms of carbazole-squaraines **M7**-**M11** and piperazine-squaraine **M12** in TBAHFP/DCM (0.2 M) at a scan rate of 250 mV s^{-1}.

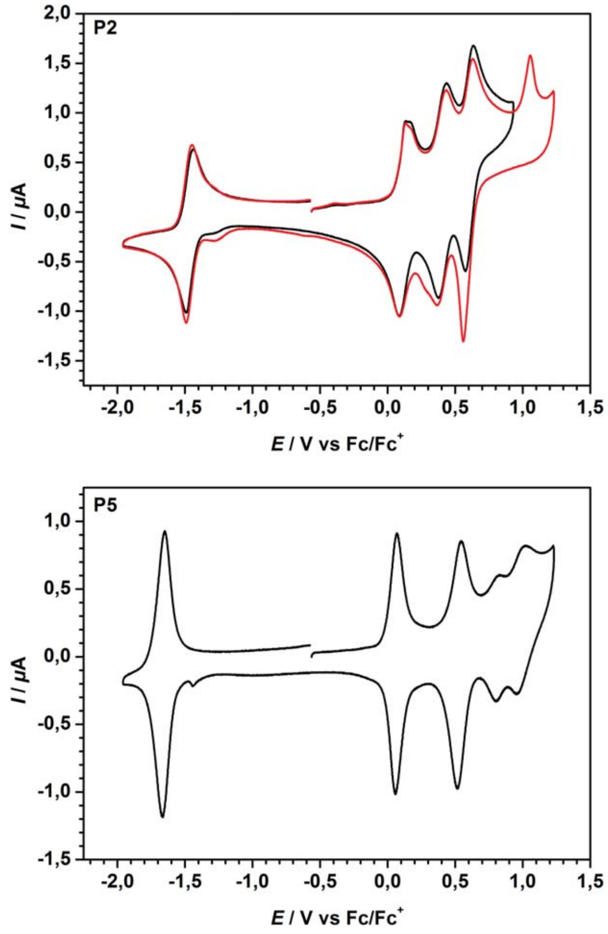

FIGURE 4 Cyclic voltammograms of **P2** and **P5** in TBAHFP/DCM (0.2 M) at a scan rate of 250 mV s^{-1}.

for the borane-squaraine conjugate **M5** we found two reduction processes far below −2 V. Differential pulse voltammetry (DPV) shows that the second of these processes covers two electron reduction. Both, **M1** and **M6** also showed an (chemically irreversible) reduction process at −2.63 V and −2.31 V, respectively. These chemically irreversible reductions are accompanied by belated back oxidation processes starting at ∼−700 mV and −400 mV, respectively (see Fig. 2). Thus, in analogy we assign the process at −1.66 and −2.49 V in **M5** to reductions of the squaraine moiety and the process at −2.65 V to the reductions of the two triarylboranes. The latter values are similar to those found in other triarylboranes.[64]

Donor Substituted Monomers

The voltammograms of the carbazole substituted dyes are depicted in Figure 3 (top: **M9**, **M10**, **M11**; middle: **M7**, **M8**). Concerning the first two oxidation steps and the reduction, only weak differences are found for squaraines linked to carbazole in either the 2- or 3-position (**M9** vs. **M10**). The *N*-linked carbazole conjugate **M11** shows both a somewhat lower reduction potential and higher oxidation potentials.

Comparison of the mono- and dicarbazole-substituted dyes **M7** and **M8**, respectively, displays that the additional carbazole decreases the oxidation potentials by around 40 mV. Scanning over a third, chemically irreversible, oxidation process leads to a different back-reduction (dotted lines). The irreversibility of the third process is likely to be due to the unprotected 3-position of the carbazoles where dimerization could occur after oxidation of the carbazole moiety.[65,66] This interpretation is supported by the third clean reversible oxidation of **M11**, where the 3,6-positions are protected by chlorine atoms and no further dimerization of the carbazole moiety is possible.

The piperazine substituted dye **M12** exhibited two clean oxidation waves (Fig. 3, bottom black line) when the scan did not include the third oxidation (red line). The third process is chemically irreversible and no clean back-reduction is detected for this process. The half wave potentials of the first two oxidation waves ($E_{1/2} = -214$ mV, 231 mV) and of the reduction ($E_{1/2} = -1.71$ V) are very similar to those of our previously published dianisylaminosquaraine dye **M15** (Chart 2) ($E_{1/2} = -190$ mV, 221 mV and −1.72 V respectively) that comprises two bisphenylamine substituents instead of two 4-methylpiperazines. The comparison indicates that the first oxidation is localized at the squaraine moiety and not at either of the substituents. In analogy to the absorption spectroscopy, this observation demonstrates the strong electron donating character of the piperazine moieties.

Homopolymers and Copolymer

The reduction and the two oxidation processes of the squaraine homopolymer **P1b** are about 30 mV at lower potential than those of our previously published homopolymer that has a higher molecular weight but is otherwise identical.[14] As mentioned in our previous work, the redox potentials were rather similar to those of the dibrominated monomeric model compound and polymerization thus has no major impact on the redox potentials.

All donor-squaraine copolymers show one reduction wave when measured in DCM. Only **P3**, which was measured in $CDCl_3$, does not show a clean reduction wave within the operating window of the solvent. Up to four oxidation waves were observed for the polymers. In case of the triarylamine-squaraine copolymers **P2** (Fig. 4, top) and **P3** (not shown), the back-reduction peak becomes distinctly sharper when a potential high enough to cover the fourth oxidation was applied. This sharp wave is a sign for adsorbed polymers on the electrode that might have precipitated at the fourfold oxidized state. In contrast, when only the third oxidation process is covered, the back-reduction shows the normal reversible signal. The voltammograms of the carbazole-squaraine copolymers **P4** (not shown) and **P5** (Fig. 4, bottom) display a very symmetric reduction wave with a small peak separation of only 20 to 30 mV. The same is true for the first two oxidation processes of **P5** (8 mV and 32 mV). We assume that these polymers adsorb to the electrode which then might lead to the observed behavior typical of thin layers where diffusion processes do not lead to the usually observed hysteresis behavior of cyclic voltammograms

TABLE 4 Absorption and Fluorescence Spectroscopic Data of Monomers (cy = Cyclohexane)

	Solvent	λ (nm)	$\tilde{\nu}_{max}$ (cm^{-1})	ε_{max} (M^{-1} cm^{-1})	λ_{fl} (nm)	$\tilde{\nu}_{fl}$ (cm^{-1})	ϕ_{fl}	τ_{fl} (ns)
M1	DCM	639	15,700	336,000	649	15,400	0.19	1.0
	Toluene	644	15,500	340,000	649	15,400	0.35	1.9
M2	DCM	642	15,600	334,000	655	15,300	0.18	1.4
	Toluene	647	15,500	327,000	658	15,200	0.46	1.8
M3	DCM	646	15,500	316,000	658	15,200	0.33.	1.3
	Toluene	651	15,400	354,000	660	15,200	0.45	–
	cy	646	15,500	244,000	657	15,200	0.41	1.7
M4	DCM	650	15,400	310,000	660	15,200	0.24	1.6
	Toluene	656	15,300	278,000	665	15,000	0.39	2.0
M5	DCM	652	15,300	432,000	665	15,000	0.30	1.7
	Toluene	655	15,300	308,000	666	15,000	0.42	2.1
M6[34]	DCM	697	14,300	217,000	719	13,900	0.40	2.5
	Toluene	711	14,100	230,000	726	13,800	0.56	4.0
	cy	720	13,900	217,000	743	13,500	0.50	3.9
M7	DCM	703	14,200	200,000	729	13,700	0.16	3.7
	Toluene	715	14,000	179,000	732	13,700	0.51	3.7
	cy	720	13,900	197,000	742	13,500	0.47	–
M8	DCM	719	13,900	233,000	742	13,500	0.14	3.7
	Toluene	731	13,700	236,000	747	13,400	0.47	3.7
	cy	733	13,600	245,000	758	13,200	0.54	–
M9	DCM	671	14,900	288,000	691	14,500	0.44	2.6
	Toluene	674	14,800	298,000	687	14,600	0.49	2.7
	cy	667	15,000	328,000	681	14,700	0.60	–
M10	DCM	669	14,900	332,000	684	14,600	0.51	2.5
	Toluene	673	14,800	355,000	684	14,600	0.55	2.5
	cy	666	15,000	294,000	681	14,700	0.58	–
M11	DCM	645	15,500	318,000	658	15,200	0.30	1.3
	Toluene	649	15,400	312,000	660	15,200	0.40	2.0
	cy	644	15,500	248,000	655	15,300	0.47	–
M12	DCM	679	14,700	188,000	710	14,100	0.03	0.19 (91.6)[a], 1.1 (8.1)[a], 6.2 (0.3)[a]
	Toluene	682	14,700	202,000	706	14,200	0.24	1.7
M13[b]	DCM	685	14,600	207,000	706	14,200	0.25	–
	Toluene	700	14,300	236,000	716	14,000	0.41	4.5
M14[c]	DCM	677	14,800	292,000	704	14,200	0.24	0.83
	Toluene	681	14,700	341,000	695	14,400	0.48	2.5
	cy	672	14,900	351,000	684	14,600	0.72	2.3
M15[c]	DCM	703	14,200	160,000	756	13,200	0.42	0.29
	Toluene	706	14,200	193,000	730	13,700	0.30	2.2
	cy	697	14,300	189,000	716	14,000	0.52	2.4

[a] The values in brackets are relative amplitudes of the corresponding lifetime.

[b] Ref. 34.

[c] Ref. 50.

under semiinfinite boundary conditions in solution. The polymerization does not have a strong impact on the potentials of **P5** as both reduction and oxidation values are in the same range as those of the model monomer **M10**. Also the potentials of **P7** do not differ very much to those of the parent monomer **M12**.

UV/Vis/NIR Absorption and Fluorescence Spectroscopy

UV/Vis/NIR-absorption and fluorescence spectra (if possible) were recorded for all compounds in two solvents. The monomers were measured in DCM and toluene, only the carbazole-series was measured in DCM and cyclohexane. If not stated elsewise, all the spectra in toluene are very

TABLE 5 Absorption and Fluorescence Spectroscopic Data of Polymers

	Solvent	λ (nm)	$\tilde{\nu}_{max}$ (cm^{-1})	ε_{max}[a] (M^{-1} cm^{-1})	λ_{fl} (nm)	$\tilde{\nu}_{fl}$ (cm^{-1})	ϕ_{fl}	τ_{fl}[b] (ns)
P1a	$CHCl_3$	739	13,500	183,000	749	13,400	0.28	1.0 (97.1), 8.1 (2.9)
	Toluene	x	x	x	x	x	x	x
P1b	$CHCl_3$	733	13,600	142,000	744	13,400	0.25	1.1 (97.0), 7.7 (3.0)
	Toluene	x	x	x	x	x	x	x
P2	$CHCl_3$	729	13,700	160,000	759	13,200	0.07	0.88 (98.7), 10 (1.3)
	Toluene	738	13,500	122,000	766	13,100	0.10	2.0 (87.3), 6.2 (12.7)
P3	$CHCl_3$	682	14,700	181,000	705	14,200	0.14	1.3 (97.4), 5.0 (2.6)
	Toluene	682	14,700	x	701	14,300	0.22	2.1 (98.6), 8.7 (1.4)
P4	$CHCl_3$	726	13,800	151,000	748	13,400	0.09	1.7 (93.1), 6.4 (6.9)
	Toluene	735	13,600	90,000	755	13,200	0.20	0.84 (31.1), 3.5 (68.9)
P5	$CHCl_3$	685	14,600	247,000	698	14,300	0.28	1.3 (97.7), 5.0 (2.3)
	Toluene	x	x	x	x	x	x	x
P6	$CHCl_3$	676	14,800	179,000	694	14,400	0.22	1.6 (94.3), 5.5 (5.7),
	Toluene	677	14,800	152,000	692	14,500	0.39	2.1 (91.6), 6.0 (8.4)
P7	$CHCl_3$	691	14,500	151,000	711	14,100	0.02	0.58
	Toluene	693	14,400	x	709	14,100	0.16	1.2 (93.4), 4.1 (6.6)

[a] The values of the extinction coefficient are per monomer unit. x = insoluble or not completely soluble.

[b] The values in brackets are relative amplitudes of the corresponding lifetime.

similar to those in DCM, only slightly shifted to lower energy. Generally the fluorescence spectra are mirror images to the main absorption bands and fluorescence quantum yields are higher in toluene than in DCM, if the compounds fluoresce at all. The polymers were measured in $CHCl_3$ and, if possible, toluene. All data of the monomers and polymers are found in Tables 4 and 5, respectively. In some cases, we also determined the fluorescence lifetime.

Squaraine Monomers

Magnified parts of the spectra of the nonfunctionalized (**M1**), functionalized (**M2**-**M4**) and triarylborane substituted (**M5**) squaraines in DCM are shown in Figure 5. All compounds in common is the typical cyanine like structure of the absorption band. A steep rise at the low energy side of the main absorption band with a huge extinction coefficient of $\varepsilon \sim 300{,}000$ M^{-1} cm^{-1} and a small shoulder caused by vibronic progression at the high energy side are the dominant features of the spectra. Nonfunctionalized squaraine **M1** has the absorption maximum at 15,700 cm^{-1} in DCM. It appears that any substituent (bromine, boronic ester, triarylborane, carbazolyl, piperazinyl) shifts the absorption maximum to lower energy. For piperazinyl this shift is strongest (1000 cm^{-1} between **M12** and **M1** in DCM), followed by the carbazolyl substituents (800 cm^{-1}). Interestingly, the position of connection of the carbazolyl substituents (**M9** vs. **M10**) does hardly influence the absorption maximum. The shift of the piperazinyl substituent in **M12** surpasses that of the recently investigated squaraine **M14** with triarylamine substituents but does not reach that of **M15** with dianisylamino substituents. Even the formal π-electron acceptor/σ-donor[67–69] substituents triarylborane (**M5**) and boronic ester (**M4**) shift the absorption maximum to lower energies as well as bromine which acts as a π-donor and σ-acceptor. For the boron containing substituents conformational issues certainly play a role which may inhibit efficient π-orbital overlap. As has been demonstrated before for **M13**, replacing one oxygen of the squaric acid moiety by a dicyanomethylene group shifts the absorption maximum of **M1** strongly to lower energy. This is also visible in the squaraine derivatives **M6-M8**. This effect is most apparent for the carbazolyl derivatives **M8** versus **M9** with a shift of 1000 cm^{-1}. The dicyanomethylene group also leads to a *cis*-configuration of the indolenine groups relative to the central squaric acid moiety while the usually most stable configuration is *trans*.[13,70]

The fluorescence quantum yield of monomeric squaraine dyes are generally higher in nonpolar toluene or cyclohexane than in DCM and range between about 20 and 60% for the series investigated here, with both **M9** and **M10** having the highest quantum yield (both ca. 60%) which again highlights that the specific position of carbazolyl attachment is unimportant for the optical properties.

The fluorescence lifetimes were recorded in the ns time regime. The samples were excited with a laser diode with a fixed wavelength at 650 nm. Fluorescence lifetimes of all monomeric squaraines are in the lower ns time regime and are all monoexponential. They are slightly larger in toluene and cyclohexane compared with DCM. Only **M12** shows three lifetimes in DCM. However, due to the low quantum yield of 0.03, the signal to noise ratio is not very good which limits the accuracy in this case.

Polymers

For the polymers we measured absorption and fluorescence spectra in $CHCl_3$ because of better solubility than in DCM, and in toluene.

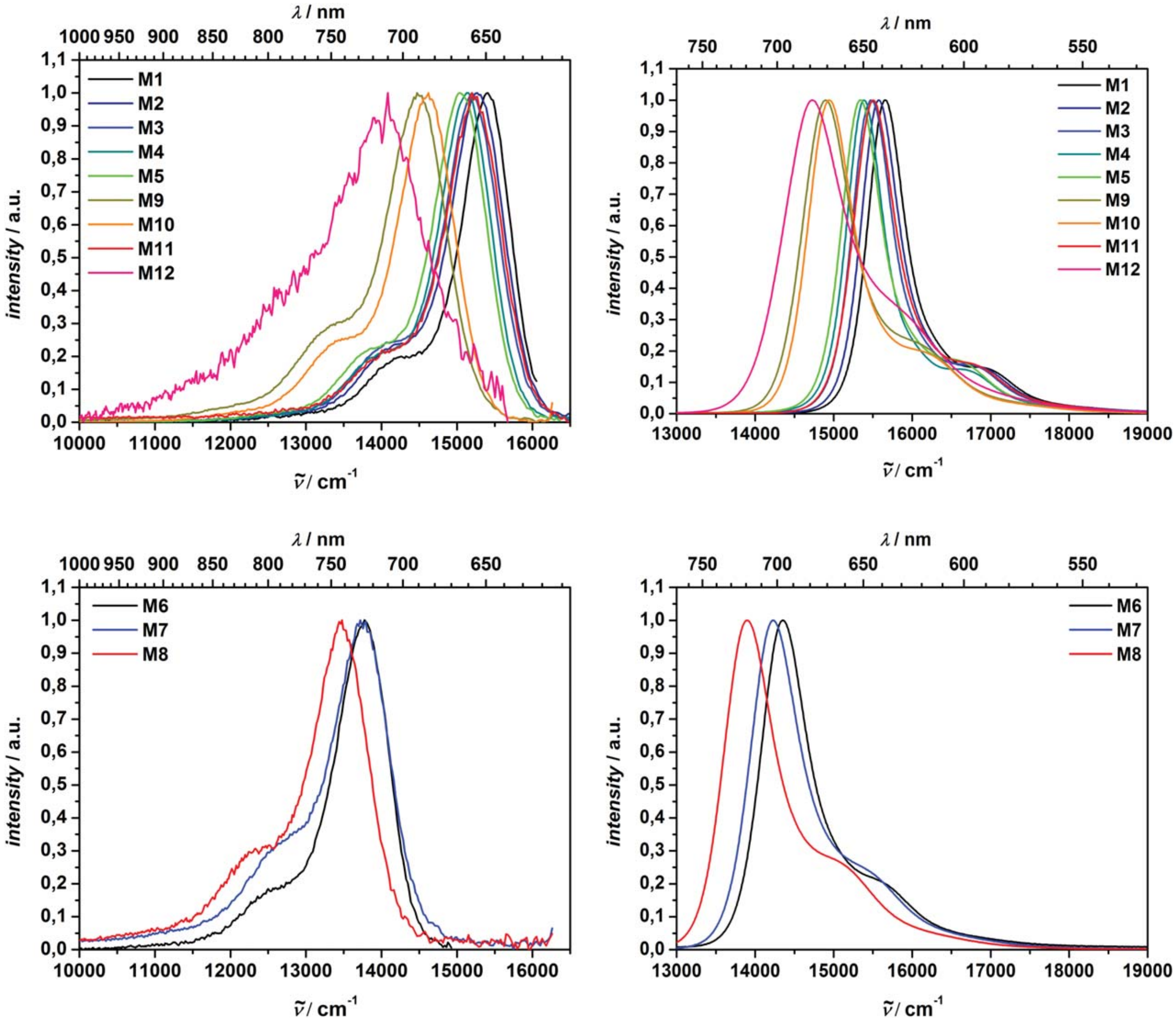

FIGURE 5 Fluorescence (left) and absorption spectra (right) of monomeric squaraine dyes **M1**-**M5**, **M9**-**M12** (top) and **M6**-**M8** (bottom).

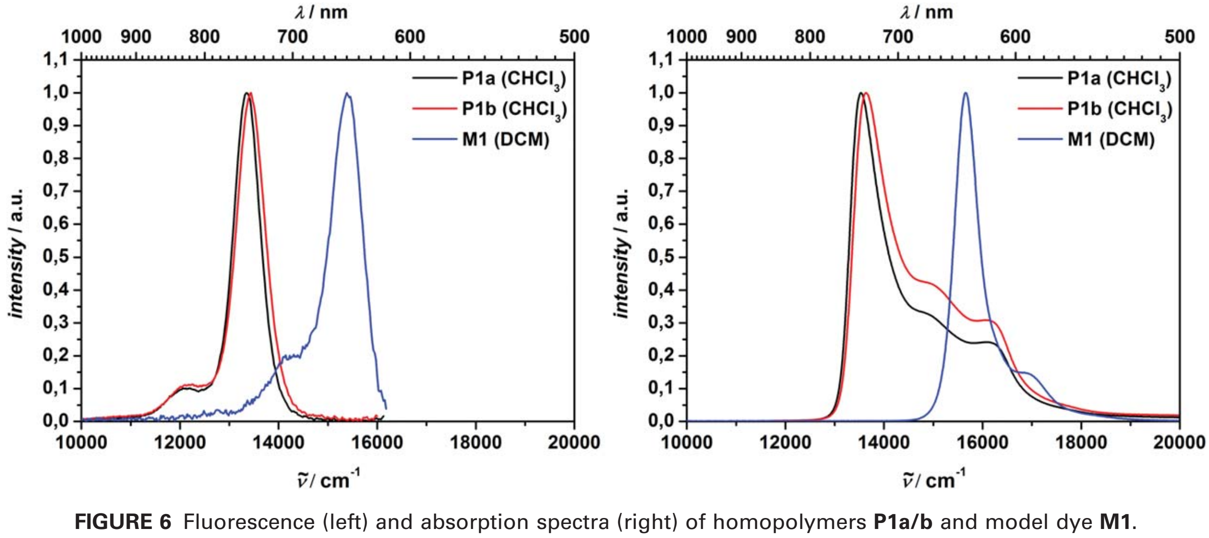

FIGURE 6 Fluorescence (left) and absorption spectra (right) of homopolymers **P1a/b** and model dye **M1**.

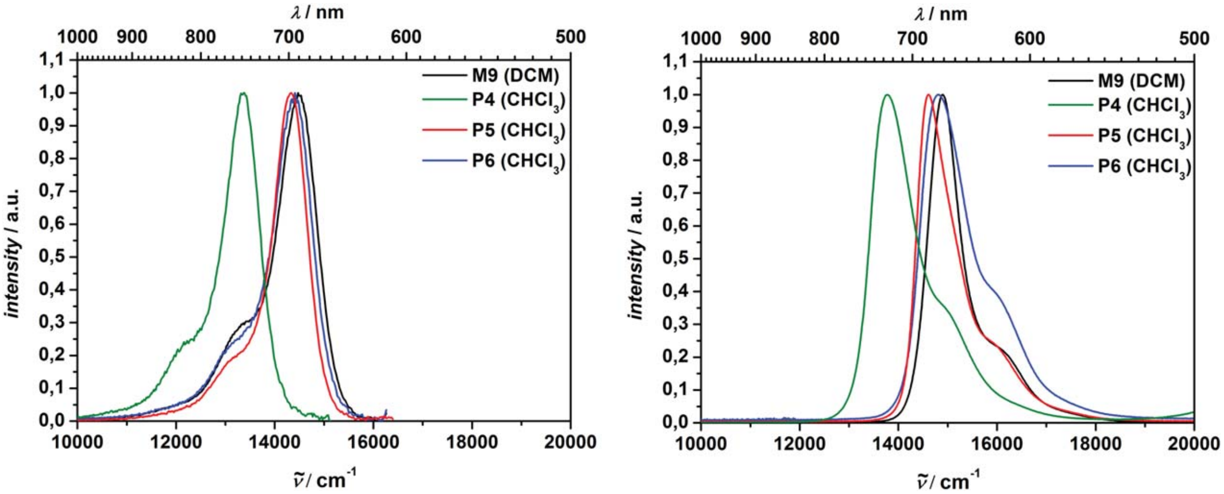

FIGURE 7 Fluorescence (left) and absorption spectra (right) of carbazole-squaraine copolymers.

Homopolymers

The homopolymers **P1a/b** show a broad main absorption band, covering a range of ~4000 cm^{-1} with a distinct intense absorption feature at the low energy side (Fig. 6, right). The broadening and the shift of the absorption compared with the monomer **M1** (~ 2100 cm^{-1}) can be explained by simple excitonic coupling of localized transition moments within the elongated polymer chains which show mainly J-type behavior (=red shifted) with some H-type contributions (=blue shifted).[11,14,34] The maximum absorption band of **P1b** is at 13,600 cm^{-1}, at only slightly lower energy than **P1a** (13,500 cm^{-1}) which shows that the effective conjugation length is reached at a degree of polymerization $X_n = 12$. However, we will show below that this simple exciton coupling model does not explain all optical features of squaraine polymers.

In contrast to the monomeric compounds, the fluorescence spectra of the homopolymers (Fig. 6, left) are no mirror images to the absorption spectra. The shape is narrower and similar to the monomeric fluorescence spectra but distinctly shifted. The Stokes shift is as small as for the monomers (100–300 cm^{-1}) and fluorescence obviously only occurs from the lowest energy excitonic state with a quantum yield of around 0.25. For the homopolymers we find biexponential fluorescence decays with both lifetimes in the low ns regime. The shorter lifetime of 1 ns is in the same range as those of the monomers and contributes with 97%. The slightly longer lifetime is around 8 ns.

Considering the better solubility of the shorter polymer and the nearly size-independent electrochemical properties (see above) of squaraine homopolymers,[14,34] the increase in length of **P1b** may only affect morphological but not electronic properties.

Copolymers

Copolymerization of a squaraine dye with either a 3,6- or 2,7-carbazole to polymers **P6** or **P5**, respectively, has hardly any impact on the absorption (Fig. 7, right) or fluorescence spectra (Fig. 7, left) compared with the model compounds **M9** and **M10**, respectively. The redshift of the absorption maxima is only 100 to 300 cm^{-1} to 14,800 cm^{-1} (**P6**) and 14,600 cm^{-1} (**P5**) and there is only little broadening of the absorption band. This indicates only little electronic coupling between the squaraine chromophores over the carbazole bridges.

The absorption band of the carbazole-dicyanomethylene squaraine copolymer **P4** is also rather narrow but at lower energy (13,800 cm^{-1}) as expected for a dicyanomethylene squaraine dye.

For the triarylamine-squaraine copolymers (**P2**, **P3**) we do also find absorption spectra that are essentially similar to the one of the monomeric dye conjugate (**M14**[50] vs. **P3**) concerning the peak with highest intensity (see Fig. 8). However, for **P3** in $CHCl_3$ there is a small but significant band at lower energy (13,800 cm^{-1}) which is absent in toluene. Polymer **P2** also shows a similar but even weaker absorption peak at lower energy (12,700 cm^{-1}) than the most intense signal. In addition, the signal at about 15,000 cm^{-1} which usually appears as a shoulder in all squaraine dyes is now more pronounced and shows a distinct peak maximum.

The copolymer of squaraine and piperazine **P7** also display an absorption spectrum that is very similar to its monomer **M12** (Fig. 9, left). But again, a low energy band of low intensity is found at 13,100 cm^{-1} both in $CHCl_3$ and in toluene. These low energy bands of **P2**, **P3,** and **P7** are plotted together in Figure 9 (right) for better comparison. The origin of these features is not fully understood but as they only appear for copolymers of squaraines with amine donors we suppose that they are caused by charge transfer interactions which only occur in some conformers, possibly in those in which the donor is coplanar to the squaraine dye. Semiempirical computations indeed suggest a lowering of excitation energy in such fully coplanar conformers, see below.

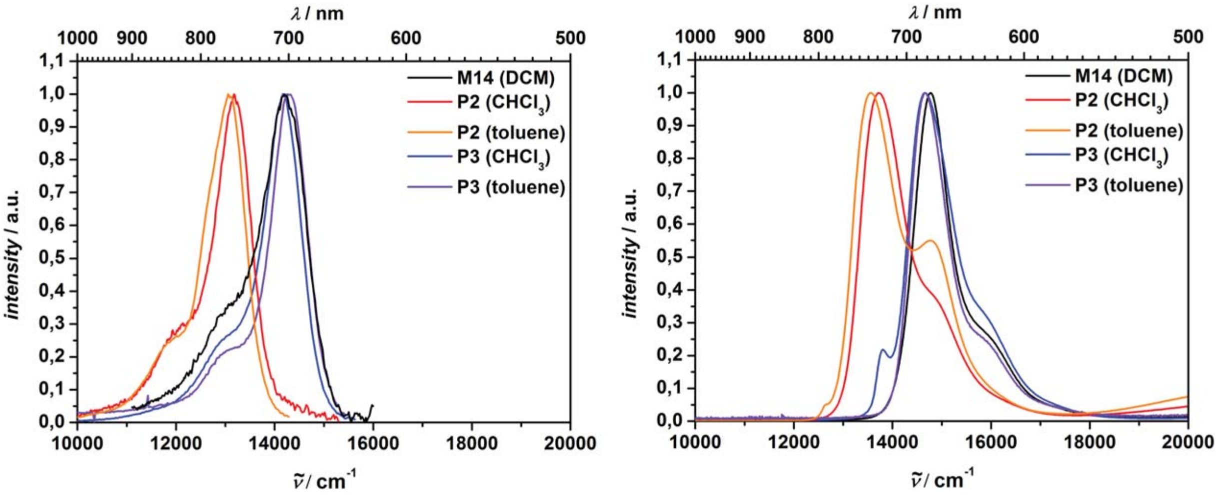

FIGURE 8 Fluorescence (left) and absorption spectra (right) of triarylamine-squaraine **M14** and copolymers **P2** and **P3** in toluene and $CHCl_3$.

The fluorescence spectra of all copolymers show essentially mirror image behavior to the absorption spectra with exception of the weak low energy band of **P2**, **P3,** and **P7** that do not show any equivalent signal in the fluorescence spectra.

The fluorescence quantum yield for **P7** (0.02 in $CHCl_3$ and 0.16 in toluene) is only slightly smaller than for the analogous monomer **M12** which is due to the saturated piperazine bridge. All other polymers however show a much smaller fluorescence quantum yield than their monomers, e.g. for carbazole copolymer **P5** the quantum yield is 0.21 in $CHCl_3$ while it is 0.51 in DCM for **M10**.

For all copolymers we find biexponential fluorescence decays. The shorter lifetimes are between 0.8 and 2.1 ns and dominate the decay with amplitudes exceeding 90%. The larger lifetimes are between 3.5 and 10 ns. However, for **P4** in toluene the larger lifetime makes two thirds of the amplitude whereas the shorter lifetime contributes with one third.

All in common is the fact that the fluorescence lifetimes of the related monomers are right between the two lifetimes of the polymers. The lifetime found for **P7** in $CHCl_3$ is unreliable because of the low signal to noise ratio caused by the low quantum yield.

To sum up, the optical behavior of all the copolymers is rather similar, no matter if the bridge is saturated (piperazine) or unsaturated, rigid (carbazole) or propeller like (triarylamine) and does not differ very much from those of the analogous monomers. These kinds of bridges obviously do not provide any significant coupling of individual squaraine chromophores by π-conjugation and the distance of chromophores is widened in such a way that exciton coupling decreases to an extent which is not noticeable.

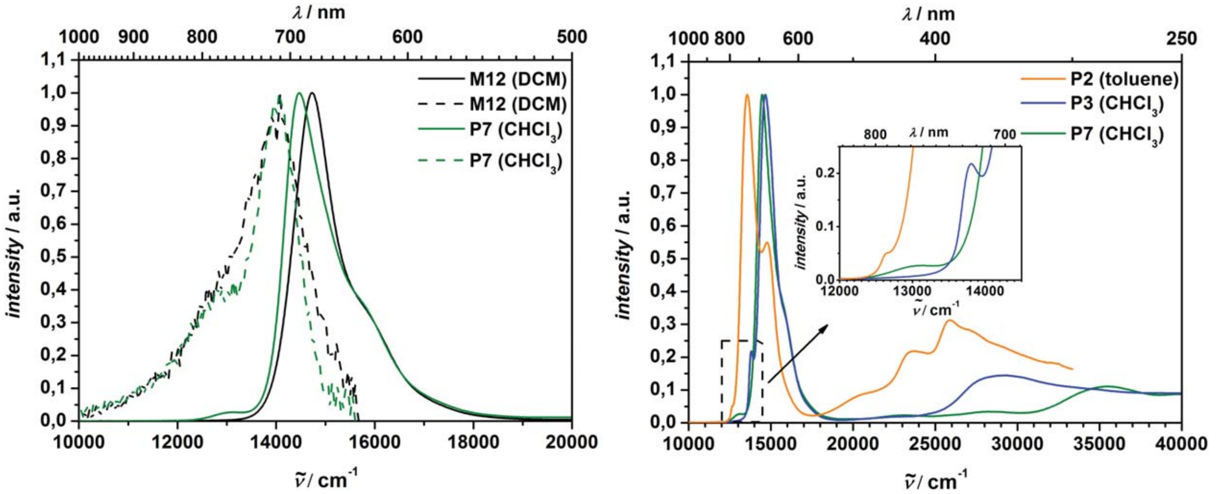

FIGURE 9 Fluorescence (dotted line) and absorption spectra (solid line) of piperazine-squaraine monomer **M12** and copolymer **P7** (left) and complete absorption spectra of donor-squaraine copolymers **P2**, **P3** and **P7** (right).

A similar behavior was reported by Kuster and Geiger for indolenine-squaraines.[46] They synthesized a series of linear squaraine dimers and oligomers and investigated the impact of various bridges. They also found only little broadening and small bathochromic shifts of the absorption bands. The induced red-shift of the bridges was in the order tetrafluorophenylene < 2,5-dialkyloxyphenylene < phenylene < fluorene. Maeda et al. bridged indolenine-squaraines via phenylene units.[45] These dyes were linked in *para*- or *meta*-positions also leading to little broadening and red-shift which was more pronounced for the *para*-linked system.

Also thiophenes were used as bridges in squaraine oligomers.[11] Much in contrast to the observations stated above, both a broadening as well as a significant red-shift was observed. The absorption maximum of a pentamer was found at 13,800 cm^{-1} in $CHCl_3$ compared with 14,900 cm^{-1} for a dithienyl substituted indolenine squaraine monomer. In contrast to phenylene bridges in the work of Kuster and Geiger (and the carbazole and triphenylamine bridges used in this study) which show a computed torsional angle of 36 to 41°, thiophene bridges may adopt a more coplanar conformation with the squaraine π-system thus enhancing π-conjugation. Semiempirical AM1 computations for model hexamers indeed gave dihedral angles of 22 to 32°, see below.

However, for *N*-alkylpyrrole squaraine dyes, significant broadening and red-shift of the absorption was reported upon copolymerization with an electron rich bridge. *Ajayaghosh* and *Eldo* used 2,5-dialkoxydivinylbenzene to bridge *N*-alkylpyrrole squaraines to form conjugated polymers with intense and broad absorption in the NIR region and low band gaps.[41,42] Into that system, Zhang et al. inserted additional donors such as thiophene derivatives, 2,7-carbazole or another 2,5-dialkoxyphenylene via the *Sonogashira* coupling and also obtained low band gap polymers with broad absorption in the NIR region.[43,44] In all these cases the conjugation pathway is provided by vinylene groups (and ethynyl groups in the latter cases) which allow for a better coplanar orientation of aromatic and heterocyclic ring moieties.

So far, as described above, the broadening and red-shift is stronger in our homopolymers **P1a/b**, where no bridges are used and the squaraine chromophores are directly linked via a C-C bond between the indolenine rings. Thus, taken together the information given above, the exciton coupling model to explain the optical properties should be modified to include conjugational effects at least in some cases.

Band Gaps

HOMO and LUMO values were obtained from the half wave potentials of cyclic voltammetry measurements. The potential of Fc/Fc^+ in TBAHFP/DCM is 0.46 eV and in TBAHFP/THF 0.56 eV versus the saturated calomel electrode (SCE).[61] Furthermore, the potential of SCE is 0.244 versus the normal hydrogen electrode (NHE), which has an absolute potential of 4.46 eV versus vacuum.[63] Therefore, in DCM $E(\text{HOMO}/\text{LUMO}) = -5.16$ eV – $E_{1/2}(1^{\text{st}}\ \text{ox}/1^{\text{st}}\ \text{red})$ and the electrochemically derived band gap is $E(\text{gap})^{\text{CV}} = E(\text{LUMO}) - E(\text{HOMO})$. In THF, -5.16 eV is replaced by -5.26 eV.

To obtain the optical band gap $E(\text{gap})^{\text{opt}}$ we used the onset of the lowest energy transition on the low energy side in the absorption spectra. Therefore we calculated the first derivation of the absorption spectra and placed a tangent at the inflexion point. The intersection point of the tangent with the *x*-axis in eV gave the optical band gap $E(\text{gap})^{\text{opt}}$.

The values of the HOMOs all are between -4.95 eV for squaraines with strong electron donors and -5.32 eV. The LUMO values are between -3.35 eV and -3.71 eV for squaraines with the strong electron accepting dicyanomethylene group in the center. The differing values for **M6** can be attributed to the THF solvent in the cyclic voltammetry measurements. The band gaps of all squaraine conjugates are between 1.52 eV and 1.88 eV. Comparison of the band gaps determined by optical and electrochemical methods shows that the latter values are 0.05 to 0.13 eV lower than the optical derived values. Only for **P1b** the optical band gap is 0.1 eV smaller than the electrochemical band gap. For **M1**, **M5** and **M6** different solvents were used for the cyclic voltammetry (THF) and the absorption spectroscopy (DCM), for this reason a direct comparison should be taken with care in these cases. Also for the polymers different solvents were used for cyclic voltammetry (DCM) and absorption spectroscopy ($CHCl_3$). However, the optical properties are rather similar for our systems in DCM and $CHCl_3$ and for this reason the band gaps are also in good agreement. In the cyclic voltammetry and absorption section above, we already discussed that no major impact on the optical or electrochemical properties is observed upon polymerization. This is also reflected in the optical and electrochemical band gaps of polymers versus monomers.

Semiempirical Calculations

In order to gain insight into the electronic structure of the polymers, the interaction of monomers and in particular the interaction with bridge molecules in the copolymers we performed semiempirical calculations. The structures of model hexamers were first optimized using the AM1 hamiltonian[71] which is known to give reliable geometries for the squaraines.[34] In all cases we used the most elongated structure that we were able to model and other conformers may have more strongly bent zig-zag structures. Although the effective conjugation length may not be reached with hexamers, it is pretty close to. In order to probe the effect of direct conjugation, we modified the dihedral angle between the squaraine monomers in the homo-hexamer and between the squaraine monomers and the bridge molecules in the copolymers. Thus, a dihedral angle of 0° will enhance conjugation, an angle of 90° will inhibit conjugation and will leave excitonic coupling—besides some hyperconjugative effects—to be the only mechanism at work for interaction. Using the thus obtained geometries, we performed CNDO/S2 calculations[72]

TABLE 6 CNDO/S2 Excited State Energies and Oscillator Strengths Based on AM1 Optimized Geometries as well as Electronic Coupling V in cm^{-1}

	Monomer[a]		Dimer[b]		Polymer optimized[c]		Polymer dihedral angle = 0°		Polymer dihedral angle = 90°	
	$\tilde{\nu}$ (cm^{-1})	f	$\tilde{\nu}$ (cm^{-1})	f	$\tilde{\nu}$ (cm^{-1})	f	$\tilde{\nu}$ (cm^{-1})	f	$\tilde{\nu}$ (cm^{-1})	f
Without bridge **P1** (**M1**)	16,678	1.79	16,500	3.92	16,437	9.79	15,997	10.39	16,817	6.67
			18,065	0.19	17,019	0.07	16,655	0.04	17,341	0.10
					17,682	0.74	17,429	0.81	17,922	0.78
					18,346	0.01	18,199	0.00	18,435	0.24
					18,886	0.32	18,823	0.35	18,831	0.91
					19,122	0.80	19,095	0.00	18,906	3.08
$V \rightarrow$			783		671		774		522	
Thiophene bridge **Py**	16,659	2.28	16,365	4.24	16,774	10.23	16,449	11.22	17,544	5.04
			17,412	0.29	17,093	0.23	16,873	0.04	17,785	0.25
					17,594	0.44	17,380	0.61	18,050	1.55
					18,002	0.03	17,876	0.04	18,316	0.20
					18,358	0.16	18,274	0.23	18,568	0.42
					18,541	1.88	18,475	0.82	18,723	4.82
$V \rightarrow$			524		442		507		295	
Carbazole bridge **P5** (**M10**)	17,105	2.35	17,211	4.44	17,828	11.30	17,532	11.74	18,331	10.45
			17,663	0.13	17,978	0.36	17,730	0.11	18,407	0.46
					18,156	0.49	17,939	0.58	18,490	0.62
					18,306	0.01	18,145	0.02	18,568	0.00
					18,452	0.22	18,316	0.20	18,630	0.12
					18,507	0.36	18,387	0.55	18,670	0.21
$V \rightarrow$			226		170		214		85	

[a] The monomer consists of the sequence bridge-squaraine-bridge.

[b] The dimer consists of the sequence bridge-squaraine-bridge-squaraine-bridge whose structure was taken from the optimization of the polymer.

[c] The polymer consists of the sequence bridge-[squaraine-bridge]$_6$.

to get the excited states. For infinitely long polymers, the nearest-neighbor approximation leads to an exciton bandwidth that is four times the electronic interaction energy V.[73] Thus, we estimated V by $(E_2 - E_1)/4$ where E_1 and E_2 are the energies of the lowest and highest excited state of the excitonic manifold, respectively. Furthermore, we assume the relative orientation of the squaraine chromophores in the model hexamers has only little influence on the electronic interaction because we investigate stretched conformers only. In these conformers the angle between the chromophores approaches 180° leading to a J-type exciton behavior for which only transitions into the lowest excited state of the exciton manifold is optically allowed. As representative examples we chose the homopolymer **P1**, the carbazole bridged copolymer **P5** and the thiophene bridged copolymer **Py** that has been investigated in form of its monodisperse pentamer by Scherer et al.[11] The AM1 optimizations gave, as expected, planar squaraines and dihedral angles between the squaraine dyes of 39 to 41° for **P1**, and between the squaraine dyes and the bridging group of 22 to 32° for **Py** and 40 to 46° for **P5**. The CNDO/S2 calculated transition energies and oscillator strengths of these model hexamers together with those of the monomers (squaraines, end-capped with two bridge units) and of model dimers are given in Table 6.

The CNDO/S2 calculations of the monomeric model compounds gave lowest energy transitions around 17,000 cm^{-1} which is about 2000 cm^{-1} too high in energy compared with experiment. This is obviously a systematic problem of the CNDO/S2 parameterization. In the dimeric model compounds, exciton coupling yields two excited states, the one being lower in energy is an allowed transition with the twofold oscillator strength, the other one at higher energy is forbidden and shows almost no oscillator strength. Half of the splitting of the two states refers to the exciton coupling V. For the model hexamers the CNDO/S2 computations gave six lowest energy transitions in a close energy range which form the exciton manifold. The lowest energy transition carries almost all of the oscillator strength which is thus about sixfold of the one of the respective monomer. This situation thus resembles a typical J-aggregate behavior. For the homopolymer **P1** the CNDO/S2 calculation predicts an only slight decrease of lowest energy compared with the monomer squaraine (see Table 6). This contrasts the experimental behavior where we found a quite remarkable red-shift of 2100 cm^{-1}. However, the calculated exciton coupling energy $V = 671\ \text{cm}^{-1}$ is in good agreement with one fourth of the experimentally observed band width (640 cm^{-1} from the peak to peak width of the highest and lowest energy peak in Fig. 6). The electronic coupling derived from the dimer ($V = 783\ \text{cm}^{-1}$) is somewhat larger which indicates that the model hexamer does not quite reach the full polymer properties concerning the full exciton band width of $4 \times V$. Artificial planarization of the polymer leads to an increase of apparent exciton coupling energy (774 cm^{-1}) compared to the one of the optimized hexamer (671 cm^{-1}) and 90° orientation between the squaraine dyes to a decrease to 522 cm^{-1}. From these values it is apparent that about 78% of the electronic coupling of the optimized polymer stems from exciton coupling interactions and the remainder from conjugation.

The situation in the thiophene-bridged **Py** is quite similar, however with a smaller electronic coupling which is about 2/3 of **P1**. The part which is caused by exciton coupling interactions drops to about 66%. In the carbazole-bridged **P5** the electronic coupling is distinctly smaller (ca. ¼ of **P1**) and again, the exciton contribution drops to 50%.

$$V_{\text{dd}} = \frac{1}{hc4\pi\varepsilon_0} \frac{\kappa\mu_{\text{D}}\mu_{\text{A}}}{r_{\text{DA}}^3} \qquad (1)$$

The decreasing exciton contribution from **P1** > **Py** > **P5** can be explained by the power-3-dependence of V on r_{DA} in the point-dipole approximation according to eq. 1[74] where $\kappa = \mathbf{e}_{\text{D}}\mathbf{e}_{\text{A}} - 3(\mathbf{e}_{\text{D}}\mathbf{e}_{\text{DA}})(\mathbf{e}_{\text{A}}\mathbf{e}_{\text{DA}})$ is an orientation factor which can be evaluated by $\mathbf{e}_{\text{D}}$ and $\mathbf{e}_{\text{A}}$, which are the unit vectors (orientation) of the transition moments μ_{D} and μ_{A} being localized at the chromophores D and A, respectively, and the vector $\mathbf{e}_{\text{DA}}$ connecting the two. $\mu_{\text{D}} = \mu_{\text{A}}$ is the transition moment of a squaraine monomer.

Thus, the CNDO/S2 calculations can explain the small changes in the carbazole-squaraine copolymer compared with the monomer model compound and the distinctly stronger coupling in **Py** and **P1**. However, the fact that both **P1** and **Py** (but not **P5**) show distinctly lower energies of their lowest transitions than the respective monomer is still unexplained. However, for all polymers, the lowest transition energy is somewhat lower for the 0° conformer than in the optimized geometry which supports the assumption that conformational issues are responsible for the small low energy peaks seen in the spectra of Figure 9, right.

It is tempting to argue that the experimentally observed missing shift of lowest energy absorption of e.g. **P5** versus **M10** is caused by a small effective conjugation length which might even be confined to only the monomer. However, even in the case of the 90°-twisted polymer where conjugation is blocked, the CNDO/S2 calculations indicate a significant exciton coupling interaction. Particularly in this case, the semi-empirical computations predict a hypsochromic shift of the allowed lowest energy transition upon polymer formation. Thus, from a missing bathochromic shift, one cannot conclude about the absence of exciton coupling interactions because the whole excitonic manifold can be shifted to higher energies, for what reasons so ever. Thus, it remains to be elucidated how the lowest energy transition within the exciton manifold depends on the degree of excitonic interaction and the degree of polymerization.

CONCLUSIONS

We followed the idea that the insertion of a strong electron donor into a polymeric squaraine system would lead to an intense and broad absorption in the NIR region. Therefore, we synthesized a series of donor-squaraine copolymers and monomeric model compounds using diverse synthetic strategies. No matter if we used transition metal catalyzed/mediated or polycondensation reactions, polymers could always be obtained in sufficient yield and molecular weight.

We investigated the impact of various bridging units on the spectroscopic and electrochemical properties. For this purpose, we chose saturated (piperazine), unsaturated rigid (3,6- and 2,7-carbazole) and propeller like (triarylamine) groups. While the absorption maxima of the model compounds generally shift bathochromically upon extension of the π-system at the periphery or the addition of donors (both σ and π), copolymerization of a squaraine dye and a donor did not have a major impact on the absorption spectra. These were only marginally broadened and red-shifted compared with the model compounds. Furthermore, the electrochemical properties remained rather similar to their monomeric model conjugates. This behavior was observed for all bridges we used. We explain this behavior to be caused by the decrease of exciton coupling energy with the power-3-dependence on the chromophore distance provoked by insertion of the bridging groups. However, conjugative effects also play a role for the interchromophore interactions and may reach about 50% for longer squaraine separations as in **P5**.

ACKNOWLEDGMENTS

This work was supported by the Deutsche Forschungsgemeinschaft within the Forschergruppe 1809 and by the the Bavarian State Ministry for Science, Research and the Arts within the collaborative research project "Solar Technologies Go Hybrid."

REFERENCES AND NOTES

1 K. -Y. Law, *Chem. Rev.* **1993**, *93*, 449–486.

2 M. Emmelius, G. Pawlowski, H. W. Vollmann, *Angew. Chem. Int. Ed. Engl.* **1989**, *28*, 1445–1471.

3 J. J. Gassensmith, E. Arunkumar, L. Barr, J. M. Baumes, K. M. DiVittorio, J. R. Johnson, B. C. Noll, B. D. Smith, *J. Am. Chem. Soc.* **2007**, *129*, 15054–15059.

4 E. Arunkumar, N. Fu, B. D. Smith, *Chem. Eur. J.* **2006**, *12*, 4684–4690.

5 M. Sameiro, T. Goncalves, *Chem. Rev.* **2009**, *109*, 190–212.

6 Z. M. Xiang, E. E. Nesterov, J. Skoch, T. Lin, B. T. Hyman, T. M. Swager, B. J. Bacskai, S. A. Reeves, *J. Histochem. Cytochem.* **2005**, *53*, 1511–1516.

7 G. J. Ashwell, J. Ewington, K. Moczko, *J. Mater. Chem.* **2005**, *15*, 1154–1159.

8 E. Collini, S. Carlotto, C. Ferrante, R. Bozio, A. Polimeno, J. Bloino, V. Barone, E. Ronchi, L. Beverina, G. A. Pagani, *Phys. Chem. Chem. Phys.* **2011**, *13*, 12087–12094.

9 Q. Q. Shi, W. Q. Chen, J. F. Xiang, X. M. Duan, X. W. Zhan, *Macromolecules* **2011**, *44*, 3759–3765.

10 S. Webster, J. Fu, L. A. Padilha, O. V. Przhonska, D. J. Hagan, E. W. Van Stryland, M. V. Bondar, Y. L. Slominsky, A. D. Kachkovski, *Chem. Phys.* **2008**, *348*, 143–151.

11 D. Scherer, R. Dörfler, A. Feldner, T. Vogtmann, M. Schwoerer, U. Lawrentz, W. Grahn, C. Lambert, *Chem. Phys.* **2002**, *279*, 179–207.

12 T. Maeda, H. Nakao, H. Kito, H. Ichinose, S. Yagi, H. Nakazumi, *Dyes Pigm.* **2011**, *90*, 275–283.

13 U. Mayerhöffer, K. Deing, K. Gruß, H. Braunschweig, K. Meerholz, F. Würthner, *Angew. Chem. Int. Ed. Engl.* **2009**, *48*, 8776–8779.

14 S. F. Völker, S. Uemura, M. Limpinsel, M. Mingebach, C. Deibel, V. Dyakonov, C. Lambert, *Macromol. Chem. Phys.* **2010**, *211*, 1098–1108.

15 S. Y. Wang, L. Hall, V. V. Diev, R. Haiges, G. D. Wei, X. Xiao, P. I. Djurovich, S. R. Forrest, M. E. Thompson, *Chem. Mater.* **2011**, *23*, 4789–4798.

16 G. Wei, S. Wang, K. Renshaw, M. E. Thompson, S. R. Forrest, *ACS Nano* **2010**, *4*, 1927–1934.

17 G. Wei, X. Xiao, S. Wang, K. Sun, K. J. Bergemann, M. E. Thompson, S. R. Forrest, *ACS Nano* **2012**, *6*, 972–978.

18 G. Wei, X. Xiao, S. Wang, J. D. Zimmerman, K. Sun, V. V. Diev, M. E. Thompson, S. R. Forrest, *Nano Lett.* **2011**, *11*, 4261–4264.

19 G. D. Wei, R. R. Lunt, K. Sun, S. Y. Wang, M. E. Thompson, S. R. Forrest, *Nano Lett.* **2010**, *10*, 3555–3559.

20 J. V. Ros-Lis, R. Martínez-Mánez, J. Soto, *Chem. Commun.* **2002**, 2248–2249.

21 J. V. Ros-Lis, M. D. Marcos, R. Martínez-Mánez, J. Soto, *Angew. Chem. Int. Ed. Engl.* **2005**, *44*, 4405–4407.

22 J. V. Ros-Lis, R. Martínez-Mánez, F. Sancenón, J. Soto, M. Spieles, K. Rurack, *Chem. Eur. J.* **2008**, *14*, 10101–10114.

23 A. Ajayaghosh, E. Arunkumar, J. Daub, *Angew. Chem. Int. Ed. Engl.* **2002**, *41*, 1766–1769.

24 C. R. Chenthamarakshan, A. Ajayaghosh, *Tetrahedron Lett.* **1998**, *39*, 1795–1798.

25 S. Sreejith, K. P. Divya, A. Ajayaghosh, *Angew. Chem. Int. Ed. Engl.* **2008**, *47*, 7883–7887.

26 J. V. Ros-Lis, B. Garcia, D. Jiménez, R. Martínez-Mánez, F. Sancenón, J. Soto, F. Gonzalvo, M. C. Valldecabres, *J. Am. Chem. Soc.* **2004**, *126*, 4064–4065.

27 S. Saito, T. L. Massie, T. Maeda, H. Nakazumi, C. L. Colyer, *Sensors* **2012**, *12*, 5420–5431.

28 L. Beverina, P. Salice, *Eur. J. Org. Chem.* **2010**, 1207–1225.

29 S. Yagi, H. Nakazumi, *Topics Heterocyclic Chem.* **2008**, *14*, 133–181.

30 A. Ajayaghosh, *Acc. Chem. Res.* **2005**, *38*, 449–459.

31 S. Sreejith, P. Carol, P. Chithra, A. Ajayaghosh, *J. Mater. Chem.* **2008**, *18*, 264–274.

32 A. L. Tatarets, I. A. Fedyunyayeva, T. S. Dyubko, Y. A. Povrozin, A. O. Doroshenko, E. A. Terpetschnig, L. D. Patsenker, *Anal. Chim. Acta* **2006**, *570*, 214–223.

33 A. L. Tatarets, I. A. Fedyunyaeva, E. Terpetschnig, L. D. Patsenker, *Dyes Pigm.* **2005**, *64*, 125–134.

34 S. F. Völker, C. Lambert, *Chem. Mater.* **2012**, *24*, 2541–2553.

35 S. H. Kim, S. K. Han, J. J. Kim, S. H. Hwang, C. M. Yoon, S. R. Keum, *Dyes Pigm.* **1998**, *39*, 77–87.

36 A. Treibs, K. Jacob, *Angew. Chem. Int. Ed. Engl.* **1965**, *4*, 694–695.

37 A. Treibs, K. Jacobs, *Liebigs Ann. Chem.* **1966**, *699*, 153–167.

38 H. -C. Lu, W. -T. Whang, B. -M. Cheng, *Synth. Met.* **2010**, *160*, 1002–1007.

39 H. C. Lu, W. T. Whang, B. M. Cheng, *Chem. Phys. Lett.* **2010**, *500*, 267–271.

40 J. Y. Wu, E. F. Huo, Z. B. Wu, Z. Y. Lu, M. G. Xie, Q. Jiang, *e-Polymers* **2007**, 077.

41 A. Ajayaghosh, J. Eldo, *Org. Lett.* **2001**, *3*, 2595–2598.

42 J. Eldo, A. Ajayaghosh, *Chem. Mater.* **2002**, *14*, 410–418.

43 W. Zhang, F. Tao, K. G. Meng, Z. Wang, L. Y. Xi, Y. Li, Q. Jiang, *J. Mater. Sci.* **2011**, *46*, 5363–5370.

44 W. Zhang, F. Tao, K. G. Meng, L. Y. Xi, Z. Wang, Y. Li, Q. Jiang, *Polym. Bull.* **2012**, *68*, 349–360.

45 T. Maeda, T. Tsukamoto, A. Seto, S. Yagi, H. Nakazumi, *Macromol. Chem. Phys.* **2012**, *213*, 2590–2597.

46 S. Kuster, T. Geiger, *Dyes Pigm.* **2012**, *95*, 657–670.

47 R. Sens, K. H. Drexhage, *J. Lumin.* **1981**, *24–5*, 709–712.

48 Innovative *Instruments*, Inc. Tampa, USA.

49 I. Noviandri, K. N. Brown, D. S. Fleming, P. T. Gulyas, P. A. Lay, A. F. Masters, L. Phillips, *J. Phys. Chem. B* **1999**, *103*, 6713–6722.

50 S. F. Völker, M. Renz, M. Kaupp, C. Lambert, *Chem. Eur. J.* **2011**, *17*, 14147–14163.

51 S. Yamaguchi, T. Shirasaka, K. Tamao, *Org. Lett.* **2000**, *2*, 4129–4132.

52 G. R. Freeman, H. A. Levy, G. M. Brown, *Acta Crysallogr. A* **1969**, *25*, S145–S146.

53 A. Midya, Z. Xie, J.-X. Yang, Z.-K. Chen, D. J. Blackwood, J. Wang, S. Adams, K. P. Loh, *Chem Commun (Camb)* **2010**, *46*, 2091–2093.

54 M. Tavasli, S. Bettington, M. R. Bryce, A. S. Batsanov, A. P. Monkman, *Synthesis* **2005**, 1619–1624.

55 D. Patra, D. Sahu, H. Padhy, D. Kekuda, C. W. Chu, H. C. Lin, *J. Polym. Sci. Part A: Polym. Chem.* **2010**, *48*, 5479–5489.

56 N. Berton, I. Fabre-Francke, D. Bourrat, F. Chandezon, S. Sadki, *J. Phys. Chem. B* **2009**, *113*, 14087–14093.

57 C. R. Chenthamarakshan, J. Eldo, A. Ajayaghosh, *Macromolecules* **1999**, *32*, 251–257.

58 Y. -Y. Chen, J. H. K. Hall, *Polym. Bull.* **1986**, *16*, 419–425.

59 A. H. Schmidt, *Synthesis* **1980**, 961–994.

60 A. Treibs, K. Jacob, *Liebigs Ann. Chem.* **1968**, *712*, 123–137.

61 N. G. Connelly, W. E. Geiger, *Chem. Rev.* **1996**, *96*, 877–910.

62 V. V. Pavlishchuk, A. W. Addison, *Inorg. Chim. Acta* **2000**, *298*, 97–102.

63 D. Tsiplakides, D. Archonta, C. G. Vayenas, *Top. Catal.* **2007**, *44*, 469–479.

64 R. Stahl, C. Lambert, C. Kaiser, R. Wortmann, R. Jakober, *Chem. Eur. J.* **2006**, *12*, 2358–2370.

65 J. F. Morin, M. Leclerc, D. Ades, A. Siove, *Macromol. Rapid Commun.* **2005**, *26*, 761–778.

66 C. J. Xia, R. C. Advincula, *Chem. Mater.* **2001**, *13*, 1682–1691.

67 C. D. Entwistle, T. B. Marder, *Angew. Chem. Int. Ed. Engl.* **2002**, *41*, 2927–2931.

68 C. D. Entwistle, T. B. Marder, *Chem. Mater.* **2004**, *16*, 4574–4585.

69 M. E. Glogowski, J. L. R. Williams, *J. Organomet. Chem.* **1981**, *218*, 137–146.

70 T. Lin, B. X. Peng, *Dyes Pigm.* **1999**, *43*, 73–76.

71 J. J. P. Stewart, MOPAC2009, Stewart Computational Chemistry, Colorado Springs, CO, USA, HTTP://openMOPAC.net, **2008**.

72 WinMOPAC, Fujitsu Ltd., 1997–1998.

73 M. Kasha, E. G. McRae, *Phys. Processes Radiat. Biol.* **1964**, 23–42.

74 T. Förster, *Annalen Der Physik* **1948**, *2*, 55–75.